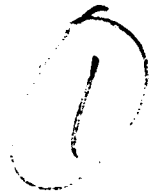

AFIT/GNE/ENP/92M-03

FEASIBILITY OF AN ANTIPROTON CATALYZED FISSION FRAGMENT ROCKET

THESIS

David S. Hidinger, Captain, USAF

AFIT/GNE/ENP/92M-03

Approved for public release, distribution unlimited

REPORT DOCUMENTATION PAGE

Form Approved
OMB No. 0704-0188

1. AGENCY USE ONLY (Leave blank)	2. REPORT DATE	3. REPORT TYPE AND DATES COVERED

4. TITLE AND SUBTITLE
FEASIBILITY OF AN ANTIPROTON CATALYZED FISSION FRAGMENT ROCKET

5. FUNDING NUMBERS

6. AUTHOR(S)
David S. Hidinger, CAPT, USAF

7. PERFORMING ORGANIZATION NAME(S) AND ADDRESS(ES)
Air Force Institute of Technology
WPAFB OH 45433-6583

8. PERFORMING ORGANIZATION REPORT NUMBER
AFIT/GNE/ENP/92M-03

9. SPONSORING / MONITORING AGENCY NAME(S) AND ADDRESS(ES)

10. SPONSORING / MONITORING AGENCY REPORT NUMBER

11. SUPPLEMENTARY NOTES

12a. DISTRIBUTION / AVAILABILITY STATEMENT
Approved for public release; distribution unlimited

12b. DISTRIBUTION CODE

13. ABSTRACT *(Maximum 200 words)*

The purpose of this project was to investigate the feasibility of an antiproton catalyzed fission fragment rocket (FFR). The FFR is characterized by the extraction of fission fragments from the fuel, and the utilization of their kinetic energy for thrust generation. A significant drawback to previous FFR designs was the required critical nuclear pile as the fission fragment source. The author examined the possibility of replacing the critical pile with a sub-critical pile driven by antiprotons. Recent experiments have revealed that antiprotons stimulate highly energetic fissions in ^{238}U, with a neutron multiplicity of 13.7 neutrons per fissions. This interaction was used as a throttled neutron source. The pile consisted of layers of fissile coated fibers which are designed to allow fission fragments to escape them, where the fragments collide with a fluid. The heated fluid is then ejected from the rocket to provide thrust. The calculations performed indicate that each antiproton injected into the pile can stimulate 8 or more fissions while maintaining a neutron multiplication of less than 0.4. Based on the results, the specific design presented was inadequate. Despite this, the concept of using the antiproton-U interaction as a source of thrust warrants further study.

14. SUBJECT TERMS
Antiproton Fission Fragment Nuclear Fission
Nuclear Rocket Spacecraft Propulsion

15. NUMBER OF PAGES
72

16. PRICE CODE

17. SECURITY CLASSIFICATION OF REPORT	18. SECURITY CLASSIFICATION OF THIS PAGE	19. SECURITY CLASSIFICATION OF ABSTRACT	20. LIMITATION OF ABSTRACT
UNCLASSIFIED	UNCLASSIFIED	UNCLASSIFIED	UL

AFIT/GNE/ENP/92M-03

FEASIBILITY OF AN ANTIPROTON CATALYZED FISSION FRAGMENT ROCKET

THESIS

Presented to the Faculty of the School of Engineering

of the Air Force Institute of Technology

Air University

In Partial Fulfillment of the

Requirements for the Degree of

Master of Science

David S. Hidinger, B.S.

Captain, USAF

March 1992

Approved for public release, distribution unlimited

Preface

Through the course of this research I have been helped by a number of people all of whom deserve my thanks. Maj Denis Beller provided encouragement, and essential knowledge and expertise. The other committee members, Col Tuttle and Maj Hartley, provided a vital sounding board, and on occasion, a much needed source of harassment. Dr. Gerald Smith, of the Pennsylvania State University, was gracious enough to spend hours on the phone relating experimental results almost as soon as he had them. In the non-technical world, my wife, Andrea, was a crucial source of support (and editorial criticism), especially after the untimely arrival of our first child, Sara. And through it all, suffering the most and complaining the least, was Jericho. I'll make it up to you buddy, I promise.

Table of Contents

Table of Figures

Table of Tables

ABSTRACT

The purpose of this project was to investigate the feasibility of an antiproton catalyzed fission fragment rocket (FFR). The FFR is characterized by the extraction of fission fragments from the fissile fuel, and the utilization of their kinetic energy for thrust generation. A significant drawback to previous FFR designs was the requirement to maintain a critical nuclear pile as the fission fragment source. The author examined the possibility of replacing the critical pile with a sub-critical pile driven by antiprotons. Recent experiments have revealed that antiprotons stimulate highly energetic fissions in ^{238}U, with a neutron multiplicity of 13.7 neutrons per fission. This interaction was used as a throttled neutron source. The pile consisted of layers of fissile coated fibers which are designed to allow fission fragments to escape them, where the fragments collide with a fluid. The heated fluid is then ejected from the rocket to provide thrust. The calculations performed indicate that each antiproton injected into the pile can stimulate 8 or more fissions while maintaining a neutron multiplication of less than 0.4. Based on the results seen, the engine design presented is inadequate. Limitations introduced by the reaction fluid far outweigh the simplicity-of-design gained. Despite this, the basic idea of using the antiproton-U interaction as a source of spacecraft propulsion warants further study.

FEASIBILITY OF AN ANTIPROTON CATALYZED FISSION FRAGMENT ROCKET

I Introduction

In the search for better methods of spacecraft propulsion, nuclear rockets of many forms have been designed. It only seems reasonable that the awesome power of nuclear fission should be quickly and easily applied to this simple task. Unfortunately, this has not been the case. Technical problems in harnessing the energy of the splitting atom and in converting this energy to thrust have, to date, been insurmountable. Many designs have been proposed, quite a few of which should work admirably, but none have been developed and used. In this paper, a spacecraft propulsion design utilizing nuclear power will be examined. It will combine features of two past designs with a startling new technology in hopes of providing an increased capability in interplanetary spacecraft performance.

1.1 Antiproton Annihilation Propulsion

The first existing space propulsion technology to be used in this new design is the matter-antimatter rocket. Because of the large amount of energy available from the antiproton ($\bar{p}$) - proton (p) interaction, this interaction is of interest in space propulsion. While the large amount of energy required to create $\bar{p}$s causes the end-to-end process of $\bar{p}$ creation and annihilation to be a net user, not producer, of energy,

it is a good energy storage method. Several authors, notably Forward, have explored the possibility of capturing the pions emitted from the $\overline{p}$ - p interaction, and then using them in various rocket designs (Forward, 1985:25-40). A major drawback to all such designs is the theoretical nature of $\overline{p}$ storage and utilization. Also lacking are the means to generate sufficient $\overline{p}$s. Further concerns arise from the methods of containing and utilizing the pions, both charged and neutral, resulting from the annihilation. The published works on $\overline{p}$ annihilation propulsion acknowledge these difficulties, and propose some possible solutions, but it may be safely said that several technological leaps will be required to utilize this propulsion scheme.

1.2 Fission Fragment Rocket Propulsion

A second proposed propulsion technology to be drawn on is the fission fragment rocket (FFR). This technology takes advantage of the high energy, heavy fragments resulting from nuclear fission. If a stream of these fragments could be directed as rocket exhaust, they would provide very high specific impulse ($I_{sp} > 1x10^6$ seconds). Using fission fragments (ffs) in this way is more efficient than allowing the fragments to stop inside the fissile material, heating it, then using this heat to deposit energy in an exhaust fluid.

Schnitzler and others investigated the possibility of using fission fragments in this way. The fission fragment source hypothesized was a large, critical nuclear pile (Schnitzler and others, 1989:1). While the idea of utilizing fission fragments as a direct energy source is attrac-

tive, a large critical nuclear assembly in space is not. A significant drawback to this configuration is difficulty in throttling the rocket. Another drawback is finding a way to direct the ffs.

1.3 Antiproton - Uranium Interaction

In the early 1980's in two experiments at the European Organization for Nuclear Research (CERN) the interaction of $\overline{p}$s with uranium was investigated. Much previous work had been done involving $\overline{p}$ interactions with protons and with some other heavy elements (Morgan, 1986:4-5). Experiments PS-177 and PS-183 were the first to use a natural uranium target for $\overline{p}$ bombardment. The results of these experiments, and further experimental and theoretical work since, have opened a wealth of possibilities for this phenomenon. It is known that the interaction of $\overline{p}$s and protons results in total annihilation of the two particles. The rest mass energy of the particles is not released as gamma rays, as is the case for the positron-electron interaction, but rather is released as pions, kaons, and gamma rays (Forward, 1985:109). When $\overline{p}$s interact with heavy nuclei, an interaction between the $\overline{p}$ and a single nucleon releases similar amounts of energy, some of which may be absorbed in the nucleus. The absorption of this energy may cause further reactions (Morgan, 1986:08). In the $\overline{p}$ - uranium interaction, the energy released within the nucleus is sufficient to stimulate fission. Fission occurs as a result of all $\overline{p}$ - U interactions (no parasitic absorption), and is fundamentally different from neutron induced fission. Due to the higher energy, and shorter lifetime of the compound

nucleus, the fission fragment spectrum is characterized by a single, relatively narrow peak, rather than the typical two peak spectrum. A larger neutron multiplicity, with higher energy neutrons also results from the $\overline{p}$ - U interaction (Smith, 1991c).

1.4 Antiproton Catalyzed Fission Fragment Rocket

If a sub-critical assembly designed after Schnitzler et al. could be used with a controllable catalyst, a throttled fission fragment rocket (FFR) would be possible. This is the principle behind the antiproton catalyzed FFR ($\overline{p}$ - FFR). Over the course of this project, the author examined the various design problems associated with this device and explored solutions to them. The main goal of the project was assess the feasibility of an $\overline{p}$ catalyzed fission pile as a space propulsion source.

II Theory

The theory behind FFRs and anti-proton annihilation rockets will be examined in this section. Existing work done by several authors will be drawn on to illustrate the concepts of these two propulsion technologies. The discussion will also involve the proposed $\overline{p}$ - FFR. The characteristics already described for $\overline{p}$ interactions with ^{238}U allow the consideration of this interesting possibility. One drawback to a traditional FFR is the requirement of sustaining a critical nuclear reactor to ensure a continuous supply of ffs. This presents many engineering and safety concerns. Further, while it is possible to regulate the criticality and reactivity of a nuclear pile, these are complex tasks. Further it is difficult to 'shut-off' and then re-start a nuclear reactor. If the production of ffs were catalyzed by $\overline{p}$s, then the pile would not need to be critical, and, as will be shown, could be easily throttled, shut down, and restarted.

2.1 Fission Fragment Rockets

The theory behind a traditional fission fragment rocket (FFR) is to cause nuclear fission inside an engine chamber and direct the fission fragments (ffs) out of the nozzle as exhaust. In terms of rocket performance, this is directly analogous to a chemical rocket which burns some fuel and releases exhaust gas out the nozzle for propulsion. One advantage of using ffs is a greater thrust per exhaust particle due to the high mass (compared to molecular gases of $A < 40$) and very high velocity ($V_e > 10^7$ m/s) of the ffs.

The primary concern in designing a FFR is the extraction of the ffs from the fuel assemblies. When created during fission these heavy, charged particles posses large amounts of kinetic energy (KE). The range of these particles in solids is very short. If the ffs are stopped in the fissile material that spawned them, their KE is left in the fissile material, and cannot be directly utilized for thrust generation. Schnitzler et al. examined the possibility of using a low density fissile core in a critical nuclear pile. The core is constructed of layers of fibers that are coated with a fissile material. A graphite filament was proposed as the fiber, with a coating of uranium carbide (UC). The energy escape fraction for this combination was calculated (Schnitzler and others, 1989:24) and the plot of this calculation is reproduced as Figure 1 (Schnitzler and others, 1989:61). Density in the proposed core is based on maintaining low enough mass thickness in each fiber layer to allow the fragments to escape that layer. Chapline specified this mass thickness to be less than 2×10^{-3} g/cm^2. Chapline further stipulated a layer separation of 20 cm, to allow the directing of the ffs out of the rocket (Chapline, 1991:1). This yields an average density in the core of 1×10^{-4} g/cm^3.

A second concern for developing a FFR is the means of directing the ffs. Having extracted some portion of the ff kinetic energy from the fibers, the ffs are then directed by magnetic fields to exhaust them from the engine. Achieving the complex field configurations to direct

the fragments is a task left unfinished in the referenced works, although some preliminary work is presented (Schnitzler and others, 1989:25).

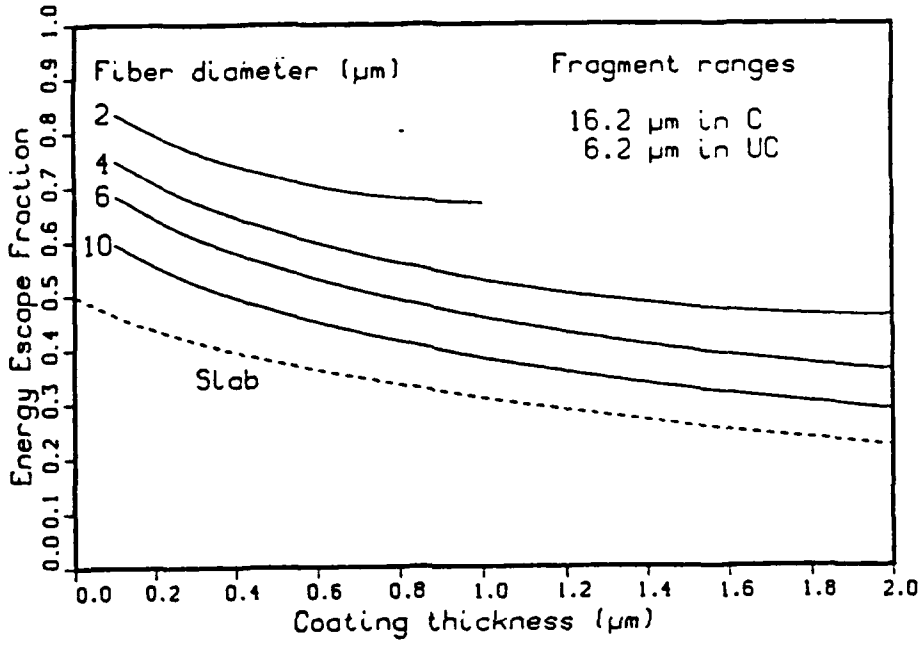

Figure 1. Fission Fragment Energy Escape Fraction (Schnitzler and others, 1989:61).

2.2 Antiproton-Catalyzed Fission Fragment Rocket

The basis of the traditional FFR is the generation of mobile fission fragments in a critical nuclear fuel assembly. The KE of the ffs is used directly as an energy source. In other reactor and engine concepts the ffs are stopped in the fuel assemblies, causing the fuel assemblies to heat up. The assemblies are then used as an energy source. In terms of rocket propulsion, Schnitzler et al. concluded that

the fission fragments themselves should serve as the rocket ejecta. The $\overline{p}$ - FFR will drastically alter the source of ffs, yet preserve the method of energy transfer, resulting in a slightly altered source of thrust for the rocket.

2.2.1 Fission Fragment Source. To generate the large number of fission fragments required, large numbers of antiprotons are required, along with a means to convert them into fissions in the sub-critical pile. In the typical missions envisioned, greater than 10^{22} $\overline{p}$s would be required.

2.2.1.1 Antiproton Utilization. Much information and speculation has been presented on the generation, storage, transport, and release of antiprotons. This work is not repeated or expanded upon here. Among the references available on this subject are Forward and Rich (Forward, 1985:5-104); (Forward, 1987:4-10); (Rich, 1989:97-113). The following assumptions are made in this study :

1. The technological capability to generate, store and transport $\overline{p}$s exists.

2. The production cost of $\overline{p}$s is a driving factor in the cost of the engine.

3. The capability to deliver $\overline{p}$s of low energy (KE < 5MeV), to a target and evenly distribute them over a surface area on the order of 10 cm^2 exists. From Lewis et al., the delivery of antiprotons to targets with dimensions on the order of millimeters is possible (Lewis and others, 1991:2).

4. The storage and handling (S&H) system is independent of, and unaffected by, the remainder of the rocket.

Based on these assumptions a neutron source will be developed for use in generating ffs.

The $\overline{p}$ S&H system must deliver the $\overline{p}$s to the PFR core via an evacuated conduit, to preclude the interaction of the $\overline{p}$s with any matter. At the end of this conduit, serving as the barrier between the vacuum and the core, will be placed a small, natural (or depleted) U target. The interaction of the $\overline{p}$s with this target serves as a neutron source. As stated earlier, when an $\overline{p}$ interacts with a heavy nucleus, it is by annihilating with one nucleon. The cross section for this interaction was computed by Morgan for high energy $\overline{p}$s. These cross sections were based on experimental data and the theory of simple geometric cross sections (Morgan, 1986:18). The curve Morgan produced, based on data from several different heavy elements, is shown as Fig 2.

At low energy, this curve is not accurate. At high energy, the geometric model is correct, because the antiproton is only mildly affected by the material, unless it does collide with a nucleus. As the $\overline{p}$ passes through a significant thickness of material, continued Coulomb interaction between the $\overline{p}$ and both the electrons (repulsive force), and the nuclei (attractive force) slow the $\overline{p}$. In effect, the $\overline{p}$ behaves like a heavy electron which scatters and slows as it passes through the material. When the $\overline{p}$ has lost most of its KE, it will be captured by a nucleus through Coulomb interaction. This effect is not

seen for high energy $\bar{p}$s passing through thin layers of material. Once captured by a nucleus, the $\bar{p}$ decays and annihilates in the nucleus. This explains the energy deposition profile Smith obtained for $\bar{p}$s in U (Smith, 1990:5). A beam of $\bar{p}$s was modeled entering a U slab. Smith found that the $\bar{p}$s deposited large amounts of energy within the slab in a narrow layer. This narrow layer represents the range the $\bar{p}$s travelled through the slab before being captured. For 6.5 MeV $\bar{p}$s, Smith found the $\bar{p}$ range in uranium to be 97 μm. This energy deposition profile is reproduced as Figure 3.

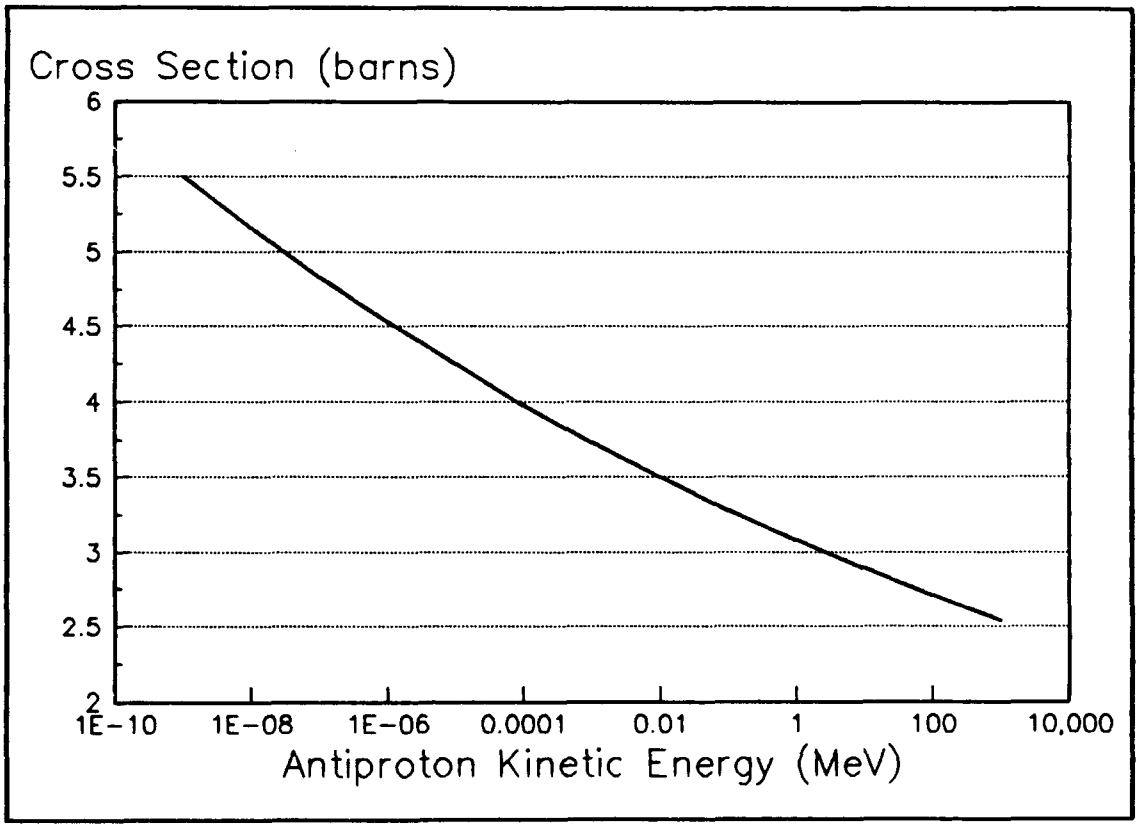

Figure 2. Antiproton-Uranium Interaction Cross Section. Plot of Equation 2 from AFRPL TR-86-011 with A=238. (Morgan,1986:18)

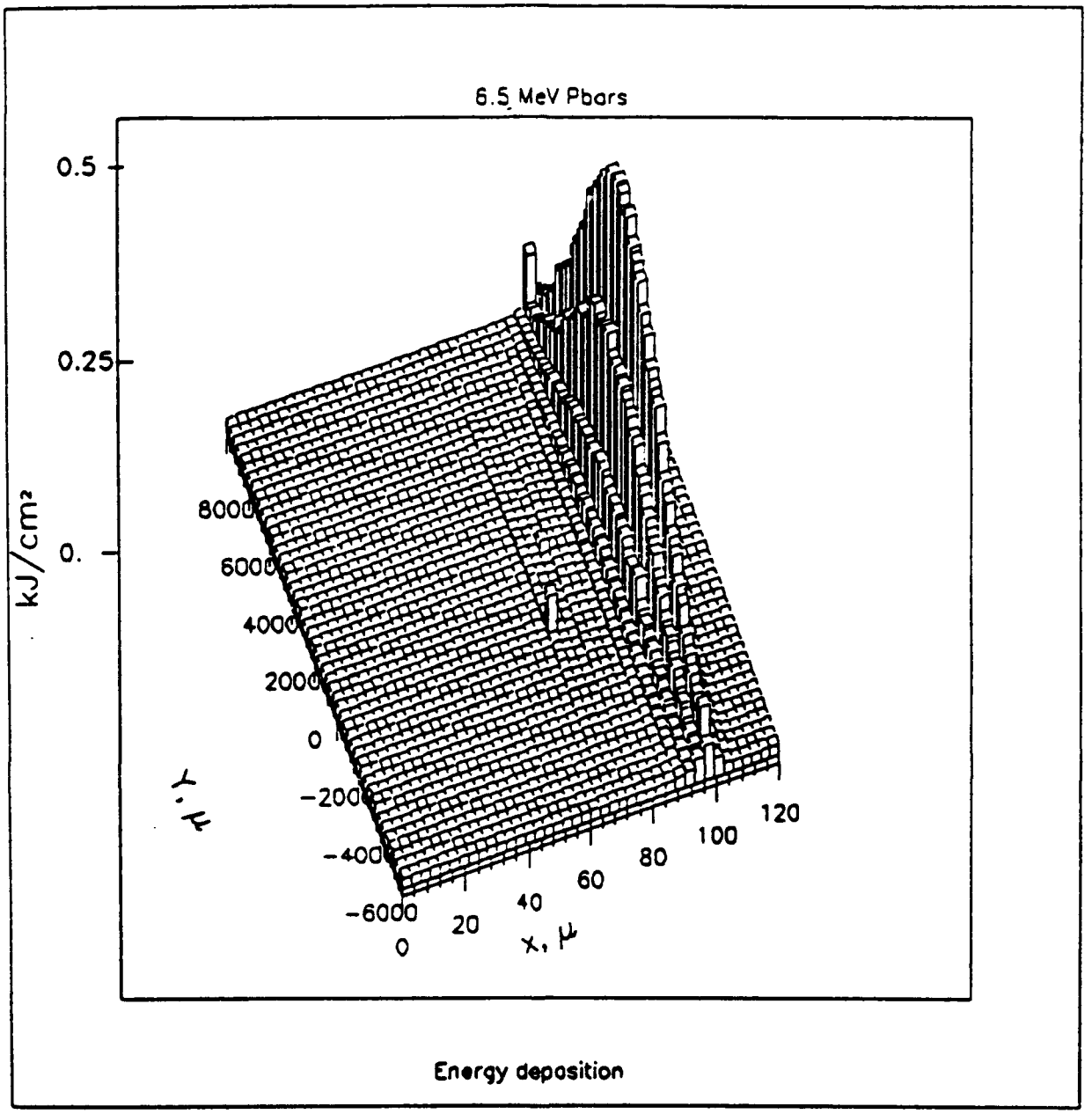

Figure 3. Antiproton Energy Deposition in a Uranium Slab. Two-dimensional energy deposition profile of 6.5 MeV antiprotons. The antiprotons travel in the direction of the x-axis, from lower left to upper right (Smith, 1990 :5).

If the U-target barrier is replaced by a thin layer of material, so as to allow the $\bar{p}$ beam into the core itself, several problems arise. First, the material used for the barrier will attenuate the $\bar{p}$ beam to some degree. And each $\bar{p}$ lost from the beam will annihilate in the barrier. These annihilations will degrade the barrier. This leads to concerns over the service life of the barrier, as it is needed to maintain the vacuum in the S&H system. Second, by introducing the $\bar{p}$s into the core, the interaction of $\bar{p}$s with the carbon fiber and the working gas is allowed. These interactions are lost from the neutron source. Third, due to the low density of the core, $\bar{p}$ ranges will be longer, and scattering from the center of the core will occur. The U-target provides a small volume isotropic neutron source -- effectively a point source. A larger, less focused source may have adverse affects on the core neutronics.

2.2.1.2 Fission Multiplication. The neutrons resulting from the $\bar{p}$ interaction with the U-target are used as a source for a sub-critical uranium pile. The purpose of the pile is to provide several ff producing fissions for each $\bar{p}$ interacting with the U-target. By using a solid U target as the neutron source, the fissions in the target do not contribute to fission fragment production. Due to the small size of the target, fission neutrons produced in it will escape with little loss to the remainder of the engine core. Here the neutrons will cause more fissions, each of which do contribute mobile fission fragments. A key element to evaluating this concept is the question of

how many fissions occur in the core for each $\overline{p}$ injected to the target.

The answer to this question is affected by a number of factors, most notably the enrichment of the uranium, the composition of the fibers, the mass of uranium present (which equates to volume of the core for constant core densities), and the reflector/moderator used, if any. It can be said that the greater the fission multiplication, the better. However, each factor affecting the multiplication does impact other aspects of the PFR design. Some guidelines used for adequate fission multiplication are: moderate enrichment, defined as not greater than 30%; fuel fiber composition of UC on graphite, with layer thickness to allow the escape of approximately 50% of the ff KE (see below); and any mass and volume required, subject to shielding size and weight limitations. The enrichment of the uranium used is limited due to the undesirable security aspects of using highly enriched uranium. While 30% enrichment is far higher than the enrichment normally found in commercial nuclear fuels (3-5%), it is still short of the enrichments of 70% or more found in nuclear weapons. This 30% guideline is arbitrary.

For the PFR concept to compete favorably with the $\overline{p}$ - p interaction, it must produce an equal or greater amount of usable energy per $\overline{p}$ injected. From Forward, it is hypothesized that a $\overline{p}$ - p rocket of the "Hot Hydrogen Gas Engine" design could utilize up to 35% of the 1876 MeV $\overline{p}$ + p rest mass energy released in each interaction (Forward, 1985:121). Forward's design will be further discussed in Section 5, but for now, the available energy per $\overline{p}$ will be used as a guide. This

available energy is about 657 MeV per $\overline{p}$. The fission fragments available from normal neutron induced fissions carry approximately 165 MeV of KE (Glasstone, 1977:12). If an energy escape fraction of 50% is assumed for the fission fragments, an energy of 82.5 MeV per fission results. To equal the available energy of 657 MeV per $\overline{p}$, a fission multiplication of 8 is required.

2.2.2 Fission Fragment Extraction. Once fissions have been generated throughout the engine core, the next task is to extract the fission fragments from the fuel assemblies, so that their KE may be used. There are two important steps in the extraction of the ffs. First, the ffs must escape the fiber where the fissions occur. Second, the ffs must escape the fuel assembly, which is the layer of fibers. Once removed from the fiber layer, the ffs will be used in thrust generation, as discussed below.

With thin fissile coatings ($\cong$ 1 μm) an energy escape fraction is achieved as depicted in Figure 1 (from Sec 2.1). A combination of 4 μm diameter fibers with a 1 μm UC coating was selected. From Figure 1, this yields an energy escape fraction of approximately 54%. Thin fibers and relatively thick fissile coatings are preferred to minimize non-fissile mass in the core. If the fiber is examined in more detail, it is found to have the properties shown in Table 1. The theoretical density of UC, 13.63 g/cm^3, is used (Yemel'yanov, 1969:149).

The mass per unit length of uranium in the fibers is approximately 84% of the total fiber mass. The total mass thickness through a fiber

is 3.6×10^{-3} g/cm^2. If the fiber layers are only one fiber thick, and the layers are separated by 2.5 cm, the average core density will be about 1.5×10^{-3} g/cm^3, or 15 times the average density used by Chapline (Chapline, 1991:1). This is possible due to the presence of fluid between the layers to stop the ffs. It should be noted that the single fiber layer will experience virtually no further loss of ff KE, while a layer of several fibers will absorb some of its own ffs.

Table 1. Properties of Fissile Fiber.

Material	Uranium Carbide	Graphite Fiber	Total
Density (g/cm^3)	13.63	2.25	----
Mass per Unit Length (kg/m)	2.14×10^{-7}	2.84×10^{-8}	3.18×10^{-8}
Mass Uranium per Unit Length (kg/m)	2.04×10^{-7}	------	2.04×10^{-7}
Transverse Mass Thickness (g/cm^2)	2.726×10^{-3}	9.0×10^{-4}	3.626×10^{-3}

To summarize, the fuel fiber layers described above allow 54% of the ff KE to escape the layers, where the energy will be utilized. The means of this utilization must differ from the methods described for the traditional FFR due to the high core density, which is caused by the smaller layer separation. Also, based on the core density and fissile content of the fibers, the engine core will contain uranium at an average density of 1.26 kg/m^3.

2.2.3 Thrust Generation. To utilize the ff KE, this energy must be transferred to the working fluid before the ffs collide with other fuel assemblies. A mass thickness of 20 mg/cm^2 is required to stop the ffs (Chapline, 1991:1). With this value, and the separation distance between fuel assemblies, the density of fluid required can be calculated. With 2.5 cm separations, the fluid density must be at least $8x10^{-4}$ g/cm^3. If He is used as the fluid at 5x normal gas density [$1.785x10^{-4}$ g/cm^3 at 0° C (Weast, 1986:B-92)], a fluid density of $8.9x10^{-4}$ g/cm^3 results. This method of energy extraction removes the need for complex magnetic fields to direct the rocket exhaust. The exhaust is now only a hot gas, and can be directed by conventional means.

By using the ffs to heat a working fluid, the average density of the rocket core has been increased. Despite the presence of the working fluid, several advantages of the original FFR concept are preserved. First, there is no requirement to build heat in the reactor core prior to use. As the ffs are produced they interact with the fluid and heat

it. If ff production is stopped, the heat source stops with little residual heat in the core. Second, the majority of reactor poisons are removed as they are produced. If the engine is shut down for a short period of time, there is little to prohibit its restart at will. These two features are crucial to achieving a throttled nuclear rocket.

III System Modeling

To evaluate the $\overline{p}$ catalyzed FFR, it is necessary to model two processes. First, the engine core is modeled to determine fission multiplication. Second, the performance of a spacecraft powered by this rocket is modeled to evaluate the rockets effectiveness.

3.1 FFR Performance Model

This was constructed by selecting several baseline engine geometries, varying the material composition of the engine, and varying the reflector used with the engine. Three configurations were then selected and used in detailed calculations. The detailed calculations were carried out with the Monte Carlo neutron transport code MORSE (RSIC CCC-203) (Emmett, 1984).

3.1.1 Engine Geometry.

The $\overline{p}$ - FFR is modeled as a right circular cylinder (RCC) of fuel coated fiber discs. This geometry is similar to that used by Schnitzler et al. (Schnitzler, 1989:60). The fuel fiber core is then surrounded by a carbon reflector, which is in turn surrounded by an aluminium support structure. A circular void of 0.5 m diameter is left in the base of the cylinder for the placement of a nozzle assembly. The volume of the core is determined by the mass of fuel to be enclosed, and the core dimensions are such that this volume is enclosed by a RCC with its height equal to its diameter. This is done to maximize volume per surface area. The reflector and support structure act as penalty weight on the engine, and are minimized when

the surface area is minimized. It should be noted that a spherical engine core would have the best ratio of volume to area. A spherical core was not used, because early in the design, the $\bar{p}$-PFR was designed to exhaust ffs. The magnetic fields needed to guide the ffs would require the axial symmetry of the RCC to allow extraction of a significant portion of the ffs. The impact of this geometry is discussed in Section 4.

To determine the volume needed, the fissile density of the core (1.26×10^{-3} g/cm^3) and required fissile mass must be known. The fissile mass required is determined by the total number of ffs to be produced, along with the enrichment of the fuel and the amount of burn-up allowed in the fuel. Fissile mass and volume will also affect the fission multiplication achieved. If it is desired to use 1×10^{23} $\bar{p}$s, at a multiplication of 10, a fuel enrichment of 25 %, and a burn-up of 1%, 156 kg of uranium would be needed in the core. This roughly corresponds to a 125 m^3 engine which contains 157.5 kg.

Given the approximate fissile mass to be used, several test cases were used to determine approximate multiplications for various geometries. From these, three cases were more completely modeled. These cases are : a 125 m^3 engine volume with a 20 cm graphite reflector (Engine #1), a 250 m^3 engine volume with a 20 cm reflector (Engine #2), and a 250 m^3 engine volume with a 10 cm reflector (Engine #3). The pertinent figures for these cases are summarized in Table 2. The structure mass listed includes the reflector and a 2 cm Al support structure. The total mass is the structure, fissile mass, and fiber mass.

Table 2. Engine Geometry Models			
Engine #	1	2	3
Engine Volume (m^3)	125	250	250
Reflector Size (cm)	20	20	10
Fissile Mass (kg)	157.5	315	315
Structure Mass (kg)	75,600	119,000	63,500
Total Mass (kg)	75,800	119,000	63,900
Core Radius (m)	2.710	3.414	3.414
Core Height (m)	5.419	6.828	6.828

3.1.2 Neutron Source. The source of neutrons in the $\overline{p}$-FFR is a stream of antiprotons interacting with the uranium target in the core. These interactions result in fission neutrons, but with markedly different characteristics than neutron induced fissions. To avoid the necessity of adding a new form of fission to the computer code used, the $\overline{p}$ - U interaction was not included in the model. Instead, a neutron source spectrum representing the $\overline{p}$-U interaction was used. Smith characterized this neutron spectrum (Smith, 1991b:2), and it is presented in Figure 5. The tabulated values used in MORSE, divided into 46 energy groups for use with the DABL69 cross section library (Ingersoll and others, 1989), appear in Table 3. These tabulated values were calculated by transforming the data table used to construct Figure 5 (Smith 1991a; 2). Note that all neutrons with energy above 19.6 MeV (the upper range of the DABL69 cross section library) are lumped into the top energy bin. These highest energy neutrons are thus more quickly thermalized in the MORSE model than they would actually be. This will lead to slightly higher fission multiplications, as these neutrons would be more likely to escape the problem prior to thermalization. Errors

due to this are assumed to be small, and are possibly mitigated by the loss of ^{238}U fissions which would have occurred from higher energy neutrons.

The uranium target is not included in the model explicitly. It is so small, relative to the pile, that it need not be modeled. For the model used, the target is placed at the center of the pile. One possible concern of using a small uranium target in this way is the heat generated inside it. Heat deposition from fission fragments will be about 165 MeV per fission.

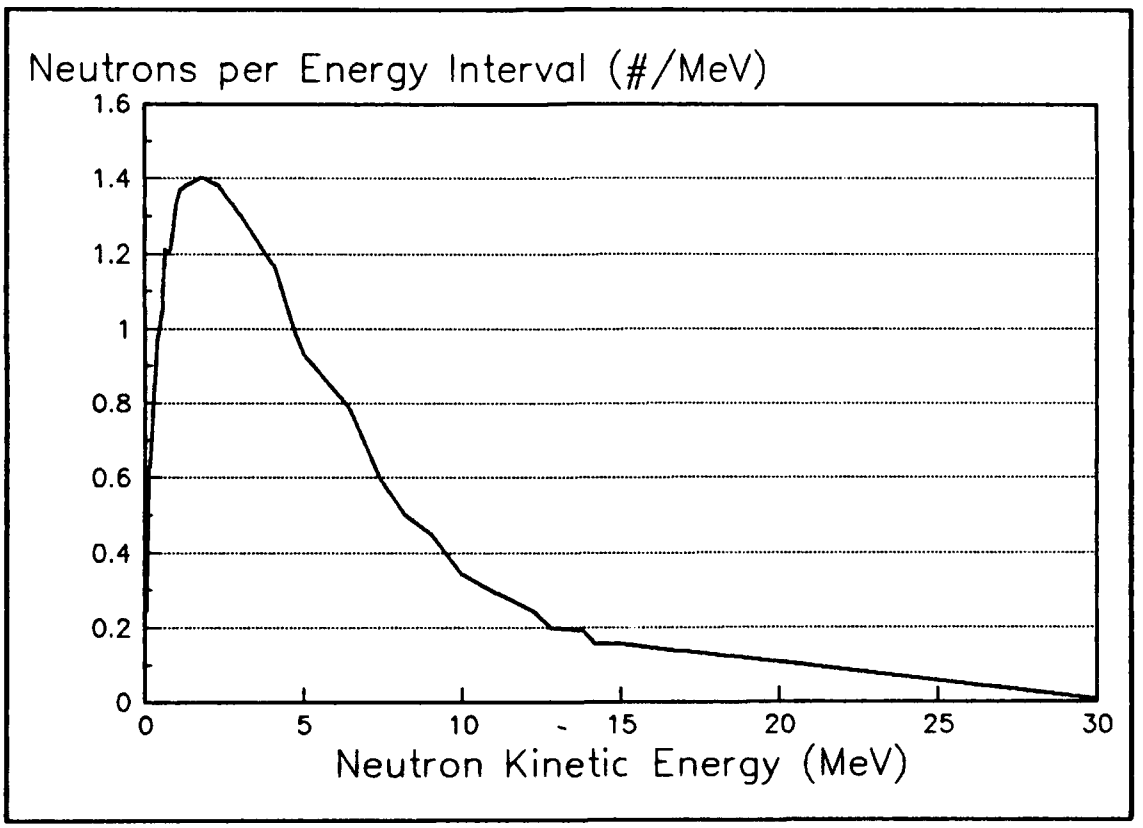

Figure 4. Neutron Spectrum of Antiproton-Induced Fission. Data taken from neutron momentum spectrum (Smith, 1991a:2).

If $1x10^{12}$ $\overline{p}$s per second are injected to the target, heat will be generated at a rate 26.5 W. If the rate of injection is increased to $1x10^{16}$ $\overline{p}$s per second, power generation jumps to 265 kW. For a small target, this amount of heat generation could be damaging. A possible solution is to cool the core side of the target with the He propellant.

Table 3 Input Spectrum of Source Neutrons for MORSE

Group Upper Energy (MeV)	Source Particles	Group Upper Energy (MeV)	Source Particles	Group Upper Energy (MeV)	Source Particles
19.6	3.61e+0	3.00	7.83e-1	5.20e-2	4.36e-3
16.9	2.75e-1	2.40	1.37e-1	3.43e-2	2.29e-3
14.9	1.11e-1	2.30	6.92e-1	2.50e-2	7.70e-4
14.2	6.36e-2	1.80	5.33e-1	2.19e-2	2.92e-3
13.8	1.93e-1	1.42	4.44e-1	1.00e-2	1.62e-3
12.8	1.20e-1	1.10	1.89e-1	3.40e-3	5.40e-4
12.2	2.72e-1	9.62e-1	1.87e-1	1.20e-3	1.53e-6
11.1	3.21e-1	8.21e-1	9.45e-2	5.80e-4	7.50e-5
10.0	3.43e-1	7.43e-1	1.25e-1	2.75e-4	4.32e-5
9.00	3.62e-1	6.39e-1	1.08e-1	1.00e-4	1.75e-5
8.20	3.99e-1	5.50e-1	1.92e-1	2.90e-5	4.40e-6
7.40	5.98e-1	3.69e-1	1.17e-1	1.10e-5	1.90e-6
6.40	1.11e+0	2.47e-1	6.64e-2	3.10e-6	4.90e-7
5.00	2.80e-1	1.60e-1	3.15e-2	1.10e-6	1.70e-7
4.70	5.97e-1	1.10e-1	3.61e-2	4.14e-7	1.00e-7
4.10	1.28e+0				

3.2 Spacecraft Mission Model

When the fission multiplication for a specific engine geometry is determined, it is possible to calculate the ideal velocity change (ΔV) achievable by that rocket. The parameter ΔV will be used in evaluating rocket performance. The ideal value used neglects the affects of drag and gravity. The calculation of ΔV is (Brewer, 1968:178):

$$\Delta V = v_e \ln\left(\frac{M_{ss} * M_{fuel}}{M_{ss}}\right)$$

where

M_f = total mass of ejecta

v_e = velocity of ejecta

M_{ss} = mass of the rocket engine and payload.

The spacecraft mission model used was generated from basic principles on TK Solver Plus (Frank, 1988), a linear problem solving package. The equations which comprise the model appear in Appendix B, along with a variable sheet which defines the terms used, and contains a sample output. To summarize the model, the following equations are solved consecutively (not simultaneously). The energy deposition rate in the FFR core is calculated:

$$\dot{E} = M * \dot{\bar{p}} * \eta_{ff} * (2KE_{ff})$$

where

$\dot{E}$ = energy deposition rate in the core

M = fission multiplication

$\dot{\bar{p}}$ = rate of antiproton injection

η_{ff} = fission fragment energy escape fraction

KE_{ff} = kinetic energy per fission fragment.

As can be seen, this depends only on the rate of $\bar{p}$ injection and the multiplication. The desired operating temperature is then used to calculate the kinetic energy per exhaust particle :

$$E_e = 1.5 * k * Temp$$

where

E_e = energy per ejected particle

k = Boltzman's constant

Temp = temperature of the ejecta.

The energy per particle can be used to calculate the velocity of the exhaust particles :

$$E_e = m_e v_e^2$$

where

m_e = mass of each ejected particle

v_e = velocity of each ejected particle.

The energy per particle is also used to calculate the number of particles needed to maintain the desired exhaust temperature for the current energy deposition rate :

$$\dot{N}_e = \frac{\dot{E}}{E_e}$$

where

$\dot{N}_e$ = rate of ejection of particles.

It has been assumed that all the ff KE delivered to the working fluid is

shared equally by the fluids particles. This amounts to an assumption of instantaneous thermodynamic equilibrium between the ffs, the fluid, the fuel assemblies, and the engine chamber. The exhaust mass flow rate can then be calculated :

$$\dot{m} = \dot{N}_e * m_e$$

where

$\dot{m}$ = mass flow rate of ejecta.

These equations are used, with a given rate of $\overline{p}$ injection and temperature in the engine chamber to calculate the mass flow rate from the rocket. For a given rocket burn time, ΔV can then be calculated. The conversion factors and intermediate equations needed are listed in full in Appendix B.

To compare the $\overline{p}$-PFR to conventional means of spacecraft propulsion two other factors must be examined. These are the specific impulse (I_{sp}), and mass ratio (MR). These are calculated by the equations :

$$I_{sp} = \frac{\dot{m} v_e}{\dot{W}}$$

where

$\dot{W}$ = weight flow rate of propellant

and

$$MR = \frac{M_{ss} + M_{fuel}}{M_{fuel}}$$

For the $\overline{p}$-PFR, I_{sp} is approximately 400 s (at T = 2570 K). Calculation of the MR will depend on the mission specified.

IV Results

Calculations of the fission pile neutronics were accomplished using the code MORSE (Emmett, 1984) on the VAX Cluster (Hercules, Starlifter, Saber, and Lancer) at the Air Force Institute of Technology. MORSE is a Monte Carlo neutron transport code. Included in the user provided inputs to MORSE are selections for the number of particles to be used in each simulation, the number of simulations to be performed to provide statistically significant results, and the weighting each particle carries both at the start of and after significant occurrences during its history. These parameters were set in an attempt to provide results with a 5% fractional standard deviation. This attempt was moderately successful. Throughout the presentation of results, error figures are given for MORSE calculated numbers. These error terms represent one standard deviation, and are generally between 2% and 8%.

Calculations of spacecraft performance were accomplished using TK Solver Plus on an IBM compatible PC. Errors from these calculations were not propagated, and are assumed to be insignificant. The error terms for fission multiplication are not carried through all calculations, for reasons that will be discussed. Overall $\bar{p}$-FFR performance was examined and compared to a hypothetical $\bar{p}$-p rocket. Performance figures are also compared to typical conventional propulsion methods. Future work which would further refine these calculations is suggested.

4.1 Fission Multiplication

The fission multiplication calculations were performed as a part of the MORSE code's basic operations. An existing output provided to the user is the weighted sum of all fissions taking place during a simulation, called FWATE. This weighted sum accounts for the variable importance of a particle throughout its time history. This output was used to provide the fission multiplication value.

While the fission multiplication in the engine core is the result of primary interest, several other results were also examined. These include the neutron fluence distribution in the core, and the criticality of the core.

4.1.1 Multiplication Curves. The fission multiplication numbers represent the average FWATE from five simulations of 1000 particles each. To translate these average FWATE values to fissions per $\overline{p}$, we must divide by the number of $\overline{p}$s injected. Since each $\overline{p}$ injected will produce 13.7 neutrons, the 1000 source particles started represent 73 $\overline{p}$s.

The three engines described in Table 2 were simulated with MORSE. For each of these simulations, a plot has been made of the fission multiplication versus enrichment of the uranium used. These plots appear as Figures 5, 6, and 7. The curve plotted represents a linear regression of the data points. Correlation coefficients for the three curves are all greater than 0.993.

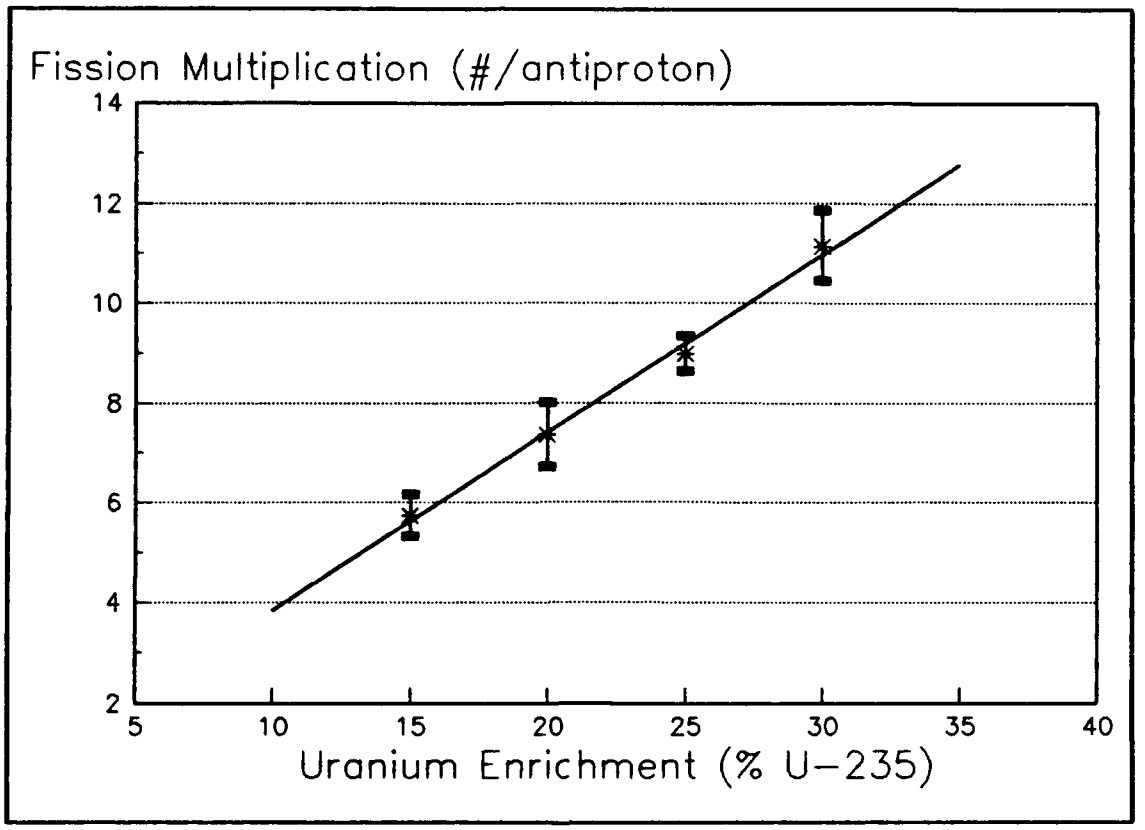

Figure 5. Fission Multiplication, Engine #1. 125 m^3 Volume, 20 cm Reflector. Error Bars are 1 Standard Deviation.

4.1.2 Engine Core Neutronics. To ensure a constant rate of fission multiplication over time, the fissions occurring in the core must be evenly distributed. This requirement for even burn-up is a principle followed in conventional reactors to maximize fuel usage, and is driven primarily by monetary considerations. In this case, even burn-up is required to ensure adequate performance of the rocket throughout its life.

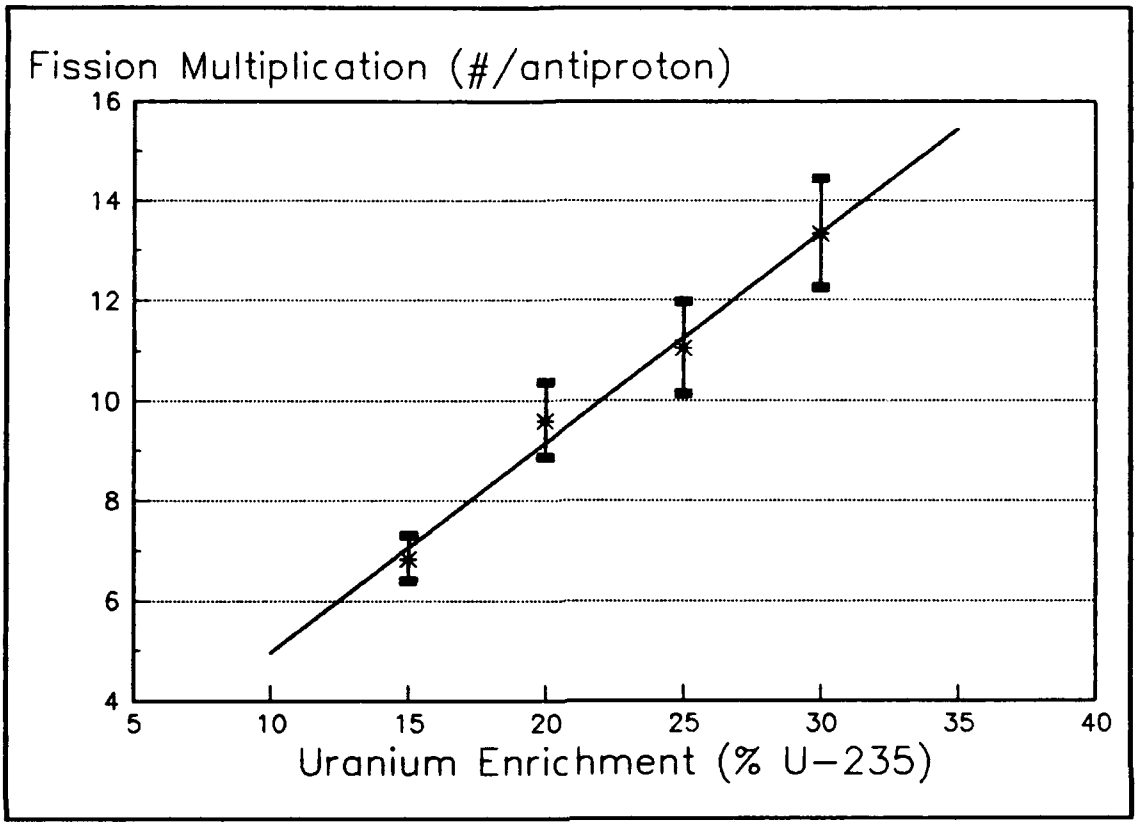

Figure 6. Fission Multiplication, Engine #2. 250 m^3 Volume, 20 cm Reflector. Error Bars are 1 Standard Deviation.

Engine size is determined by the number of ffs to be produced, and the amount of burn-up to be allowed. We will limit the burn-up of our engines to 1% of the U-235 present. For the 125 m^3 Engine #1, with 25% U-235 enrichment, this yields a maximum of $1x10^{24}$ fissions for 1% burn-up. It is assumed that with an evenly distributed 1% burn-up no change occurs in the neutronics of the pile or in the fission multiplication.

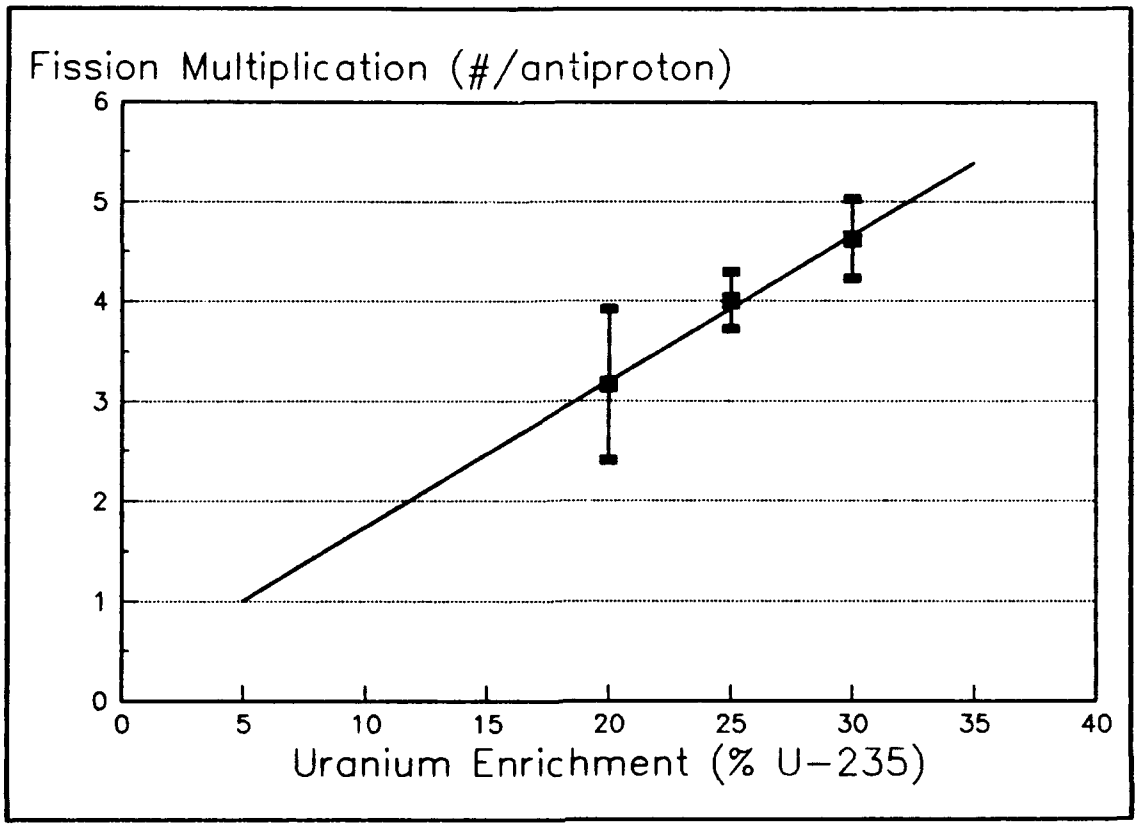

Figure 7. Fission Multiplication, Engine #3. 250 m^3 Volume, 10 cm Reflector. Error Bars are 1 Standard Deviation.

A measure of the distribution of the burn-up in the pile is the distribution of the neutrons. The two are proportional because the reaction cross sections are the same throughout the core. To measure the neutron distribution, two existing FORTRAN sub-routines, TRKBDR and TKRCOL, were modified and used (Cramer, 1985:49-52). These subroutines use the standard MORSE routine FLUXST to sum the path length travelled by each particle throughout its history, and store the result in a detector array (Cramer, 1985:35). The final results are then provided as total path length per source particle for each detector. The modi-

fied subroutines and the user provided FORTRAN code appear in Appendix A. If the volume of each detector is known, this information may be used to provide the track length (n-cm) per volume (cm^3). This results in the neutron fluence (n/cm^2) per source particle, for each detector.

To determine the fluence distribution in the $\bar{p}$-FFR Engine #1, with 25% enriched fuel, was divided into 10 detector zones. The first zone was a cylinder at the center of the engine, the volume of which was 12.5 m^3. The remaining detectors were placed around the first in the form of concentric cylindrical shells, each having a volume of 12.5 m^3. The measured fluence distribution for this configuration appears in Figure 8. The same engine configuration was then divided into 10 detector discs, each of 12.5 m^3 volume. The measured fluence for this configuration appears in Figure 9.

As has been stated, it is desired to maintain the $\bar{p}$-FFR as a subcritical pile. To ensure this, MORSE was used to calculate k_{eff}, the effective neutron multiplication from one generation to the next. These calculations were accomplished for engine configurations #1 and #2 with enrichments of 25%. The MORSE input files used for these calculations are included in Appendix A.

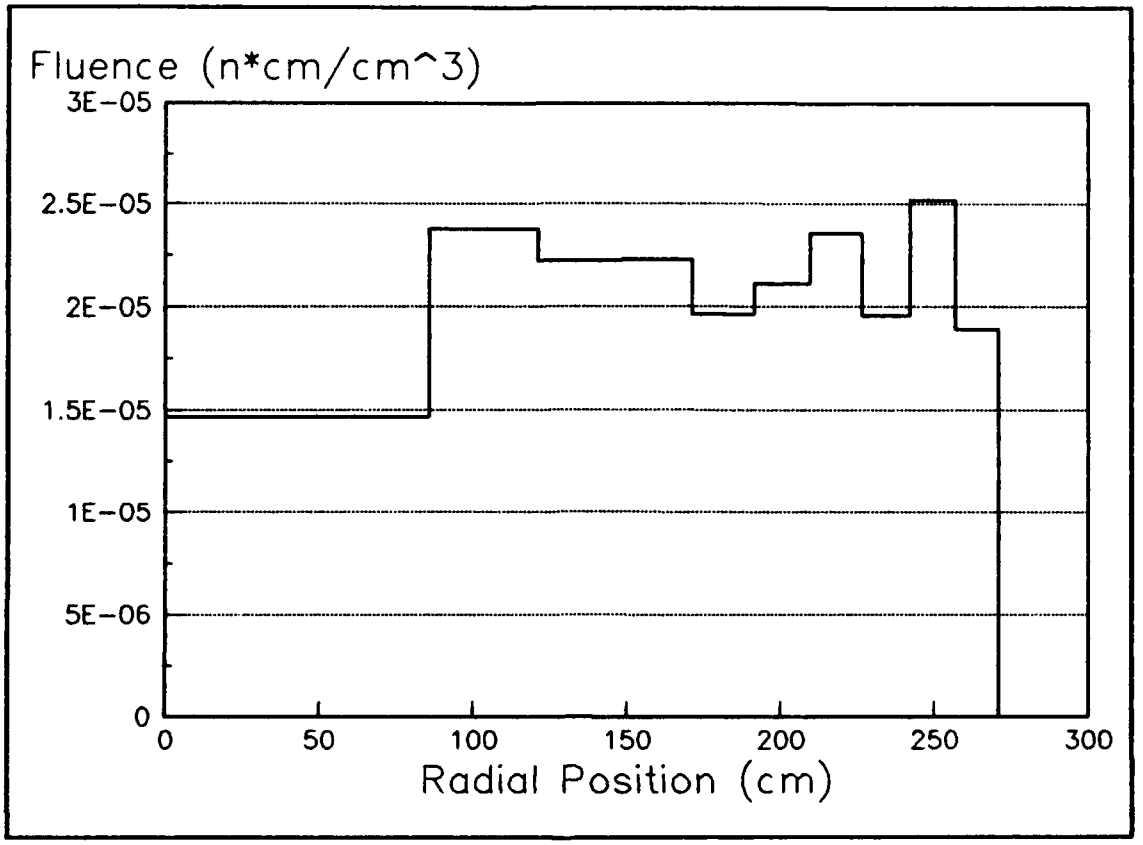

Figure 8. Radial Dependence of Neutron Fluence in the FFR Core. Engine #1, 25% Enriched UC. Error Bars not Shown, First Standard Deviation for all Data Points < 2%.

For engine #1 the MORSE calculation provided the result k_{eff} = 0.334 ± 0.008, and for Engine #2 k_{eff} = 0.380 ± 0.014. In both cases these figures show that the pile is far sub-critical, in keeping with the design goals.

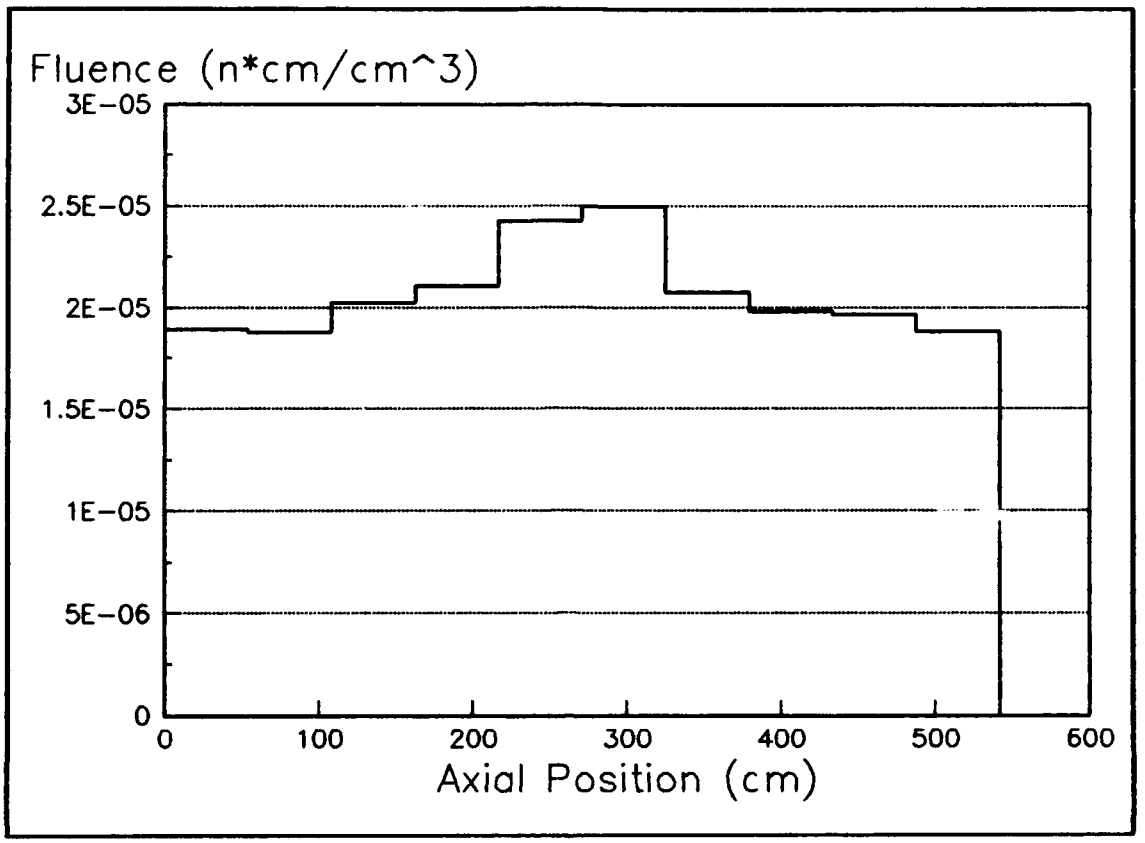

Figure 9. Axial Dependence of Neutron Fluence in the FFR Core. Engine #1, 25% Enriched UC. Error Bars not Shown, First Standard Deviation for all Data Points < 3.6%.

4.1.3 FFR Design Parameters As was discussed in Section 2.2, a fission multiplication of 8 allows the $\bar{p}$-FFR to generate energy at a rate similar to a $\bar{p}$-p rocket. To achieve this level of multiplication with the engine geometries used, enrichments of less than 25% are required. This allows some latitude in the design parameters of size and shielding.

The statistical uncertainties associated with the multiplication figures are not carried through the spacecraft performance calculations because of this latitude. The multiplications used are intended as an estimate of actual engine performance. If the multiplication for an engine geometry is lower than that calculated, it can be boosted by increasing the fuel enrichment slightly. The k_{eff} values calculated show that a small increase in enrichment will still meet the design goal of a sub-critical pile. A small increase in fuel enrichment does not affect any other performance parameter, and only affects the final spacecraft ΔV by changing the multiplication.

4.2 Spacecraft Delta V Calculations

As can be seen from the equations used in the spacecraft performance model, three variables affect the final results for ΔV. These are m_e, the ejecta mass; T, the ejecta temperature, (or ejecta velocity, any two of the three); and Npbar, the total number of $\bar{p}$s. In calculating the thrust delivered, pdot, the injection rate of $\bar{p}$s is also important. But for ΔV, the length of time used to deliver Npbar $\bar{p}$s does not matter. While the mission time does not affect ΔV, it may affect mission planning. Thrust times of greater than 10 years will be considered undesirable. Of these variables, m_e is decided by chemistry, as will be discussed. The calculations performed then fall into two categories. First, the exhaust temperature was fixed, and a plot of ΔV vs Npbar was generated. Second, Npbar was fixed and a plot generated of ΔV vs T.

For the plot of ΔV vs Npbar, two values of pdot were used, $1x10^{12}$ and $1x10^{16}$ $\bar{p}$s per second. Exhaust temperature, T, was fixed at 2570 K. Values of Npbar ranged from $1x10^{22}$ to $3x10^{26}$. With a $\bar{p}$ injection rate of $1x10^{16}$ $\bar{p}$/sec, this corresponds to thrust times of from roughly 12 days to 950 years. This plot appears in Figure 10.

To examine the affect of exhaust temperature on ΔV, the same value of pdot was used, and Npbar was fixed at $1x10^{24}$. Temperatures ranging from 1000 K to 4000 K were used. The results of this calculation appear as Figure 11.

4.3 FFR Performance

The physical performance of the nuclear pile can be evaluated based on the results described in Sections 4.1 and 4.2. These results show that the $\bar{p}$-FFR provides the number of fissions desired, and in doing so, remains sub-critical. The neutron fluence in the core was also calculated. As can be seen in Figure 9, the axial neutron fluence is slightly peaked at the center of the pile. This peak is 133% of the lowest fluence seen. With this fluence distribution, when the low fluence region has reached a 1% burn-up, the center of the core will have reached a 1.33% burn-up. This is not a concern. Examining the radial fluence distribution in the same manner shows a peak fluence that is 172% greater than the lowest fluence. At a burn-up of 1%, this difference is not a concern. When the low fluence region has reached its 1% burn-up, the high fluence region will retain 98.28% of its ^{235}U.

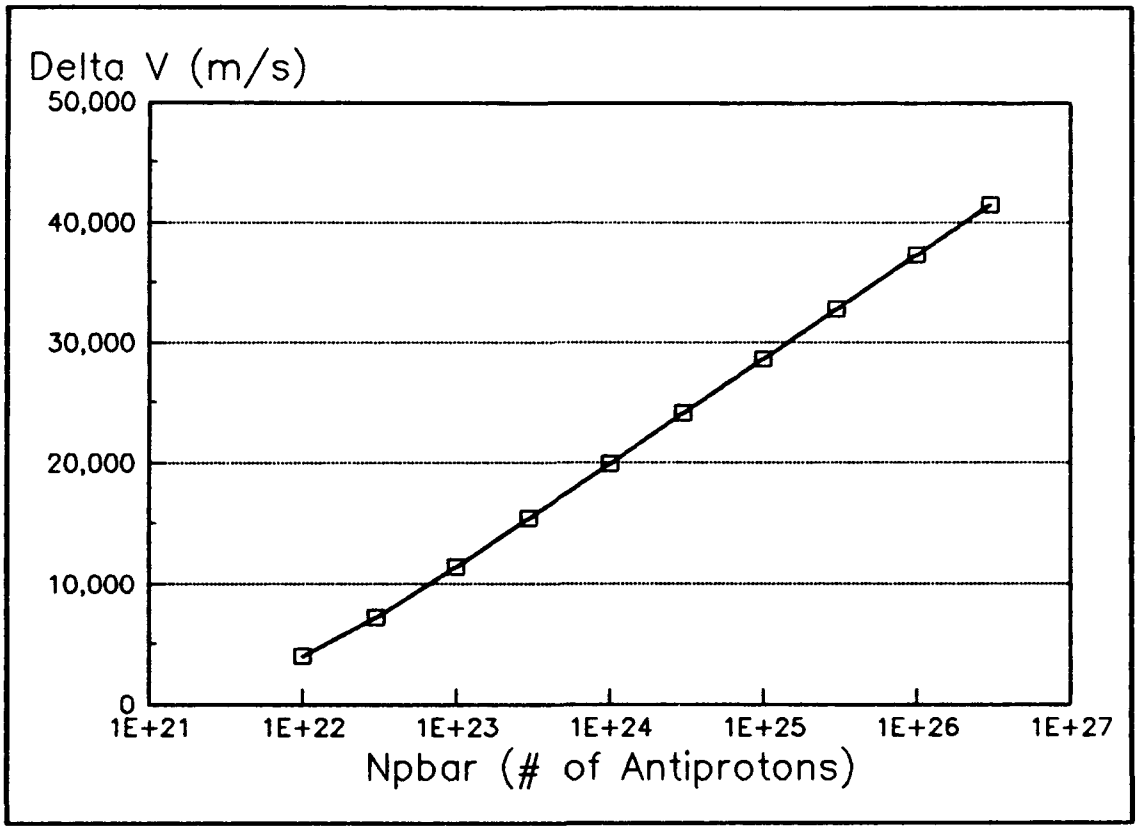

Figure 10. Velocity Change Versus Number of Antiprotons.

At this point we will compare the catalyzed FFR to the $\overline{p}$ - p annihilation rocket. The Hot Hydrogen Gas Engine (HHGE) proposed by Forward consists of a large pressure vessel contained in a magnetic field. The vessel is filled with hydrogen, and $\overline{p}$s are fed into it. As the $\overline{p}$s interact with the hydrogen, the magnetic fields are used to contain the resulting charged pions. The pions then collide with the hydrogen, transferring their KE. Forward hypothesized transferring 35% of the $\overline{p}$ + p annihilation energy to the hydrogen. The hydrogen is then exhausted from the rocket to produce thrust (Forward, 1985:121-123). In terms of

rocket performance the only difference between the two designs ($\overline{p}$-FFR and HHGE) are the choice of working fluid and the exhaust temperatures achievable.

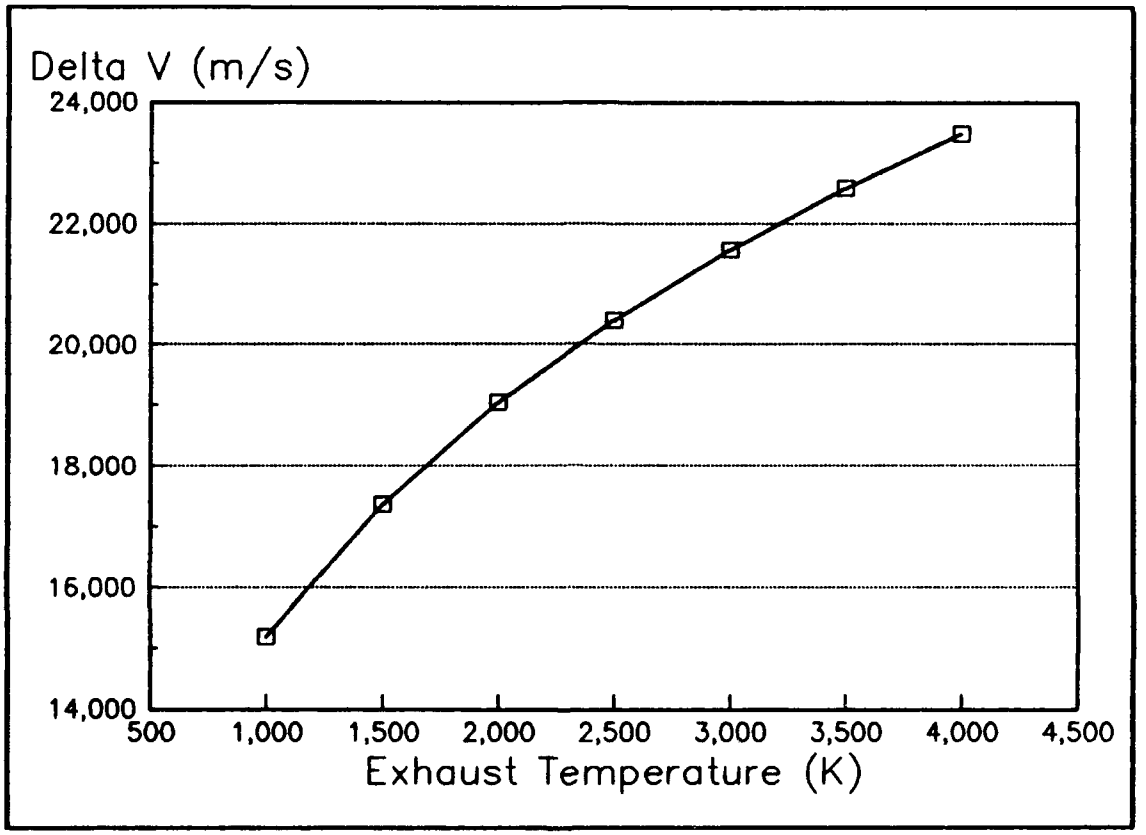

Figure 11. Velocity Change Versus Exhaust Temperature.

For the $\overline{p}$-FFR, the use of unclad fuel assemblies (fibers) limits our choices of working fluids. Uranium is reactive with hydrogen, even in the uranium carbide compound (Yemel'yanov, 1969:147). While references were not found for high temperature (T > 2000 K) reactions, it will be assumed that hydrogen is not suitable as a working fluid. The next best choice is Helium, as we desire as light a fluid as possible. Helium is an appropriate choice, as no interaction with uranium or ura-

nium carbide is noted, unless the Helium is contaminated with oxygen, nitrogen, or water vapor (Yemel'yanov, 1969:147). The HHGE uses hydrogen as a working fluid.

A direct comparison of the $\overline{p}$-FFR and HHGE is difficult. Forward did not calculate the ΔV achievable by an HHGE, but he did provide the essential information to do so (Forward, 1985:123). Missing from the data provided is the vehicle mass required to support the HHGE. This mass will be assumed to be 10,000 kg with a 5,000 kg payload. Using the figures for mdot, pdot, and exhaust temperature provided, the spacecraft mission model was adapted to calculate ΔV for the HHGE. A total mass 120 mg of $\overline{p}$s (7.22×10^{22} $\overline{p}$s) is used, propelling this spacecraft to 23.6 km/s. A similar computation, using Engine #1, 7.22×10^{22} $\overline{p}$s, and a 5000 kg payload yielded a ΔV of only 10.6 km/s. Both calculations are summarized in Table 4.

Table 4. Spacecraft Mission Comparison

Spacecraft	HHGE	$\overline{p}$-FFR
Payload (kg)	5,000	5,000
Total Mass (kg)	15,000	81,737
Exhaust Temperature (K)	3,700	2573
Ejecta Mass (kg)	160,000	1,070,000
ΔV (km/s)	23.6	10.4

From Table 4, it can be seen that the HHGE uses the available $\overline{p}$s more efficiently in propelling the spacecraft. This is despite the fact that the available energy per $\overline{p}$ is about the same. This is

attributable to two sources. The first source is the obvious discrepancy in total vehicle mass. This is difficult to evaluate, as Forward does not provide any vehicle mass figures for the HHGE. Forward does hypothesize a 10,000 kg vehicle with payload included (Forward, 1985:131), but its high exhaust temperature (T = 14,000 K) indicates that it is not the HHGE.

The second source of discrepancy is the exhaust velocity attainable by the two rockets. Exhaust temperatures in the HHGE rocket are limited by the material properties of the tank and nozzle used. Both these structures can be cooled, and any material desired might be used. For these reasons, fairly high temperatures are reasonable. In the FFR concept, temperatures are limited by the assumption of thermodynamic equilibrium between the working fluid molecules, engine chamber walls, and fuel fibers. Because of the necessity of extracting the ffs, we cannot clad the fuel fibers. Therefore, they are limited to temperatures below 2623 K, the melting point of UC (Yemel'yanov, 1969:145)

To compare the $\overline{p}$-FFR to other propulsion systems the parameters I_{sp} and MR are used. The mission shown in Table 4 would have the characteristics I_{sp} = 408 sec, and MR = 140. This I_{sp} is better (higher) than most conventional fuels, which fall in the range 200 - 300 s (Brewer, 1968:149). The MR given is high, but according to Forward is compatible with storable chemical rockets for this type of mission (Forward, 1985:134).

In terms of energy storage, the $\overline{p}$-FFR uses 157.5 kg of U, and a negligible mass of $\overline{p}$s to generate up to 8.9×10^{25} MeV from 1×10^{24} fissions. This calculation does not include the initial $\overline{p}$-U interaction, or the 46% ff KE lost. Equivalently, 157.5 kg of TNT contains approximately 4.5×10^{21} MeV (Glasstone, 1977:13).

4.4 Future Work

The work presented in this paper was conducted as a feasibility assessment of the $\overline{p}$-FFR. To fully evaluate the concept further work would be needed. A summary of some of the effort required follows.

4.4.1 Modeling improvements. The model developed for the performance of the $\overline{p}$ catalyzed fission pile can be best improved in two areas. The first is the treatment of high energy source neutrons. The available neutron cross section library, DABL69 was developed for use with fission and fusion models. For this reason, it has an upper energy cutoff of 19.6 MeV. The $\overline{p}$-U interaction yields neutrons with considerably more KE than this. In this paper, these neutrons were placed in the highest available energy group, with an unknown affect on the calculations fidelity.

The second area for improvement is the thermodynamics in the pile. Energy transfer from the fission fragment to the working fluid was assumed to be in the form of instantaneous thermodynamic equilibrium. This equilibrium was extended to the fuel assemblies, limiting exhaust temperatures to the melting point of the assemblies. Energy deposition

in the fibers by fission fragments was not modeled, and energy deposition in the uranium target by the $\bar{p}$s was only briefly treated. A better understanding of the thermodynamic processes in the pile will yield more accurate results and design limitations.

4.4.2 Design Improvements. The proposed design of the $\bar{p}$-FFR could also be improved. Among the design changes might be : improvement of the engine geometry; increase in fissile mass in the pile; improvement of the working fluid; and elimination of the working fluid.

By using a spherical geometry, the surface-area-to-volume ratio would be decreased. This would lead to less reflector mass for a given engine volume. For Engine #2, the use of spherical geometry would reduce the structure mass to 102,000 kg, a 14% reduction. The effect of this new geometry on the core neutronics is unknown.

Performance would be improved in two ways by reducing the diameter of the graphite fibers used in the core. First, the fission fragment energy escape fraction will increase. The current configuration of 4 μm fibers with a 1 μm fissile coating yields an escape fraction of 54%. By reducing the diameter of the fibers to 2 μm, this fraction increases to 73%. Also, the reduction in the size of the fibers increases the percentage of fissile mass in the core. The requirement to allow the ffs to escape the fiber layers limits the average core density. A greater fraction of this density devoted to fissile mass would allow a smaller

core to contain the same amount of fissile material. A smaller fiber diameter was not used due to uncertainties in the thermal response of the fiber.

The most easily attained performance increase would come from replacing the He in the core with H. This lighter fluid would increase thrust and ΔV. As was stated in the paper, the affects of H on the UC at high temperature is unknown.

If the working fluid were eliminated, the $\bar{p}$-FFR would more closely resemble the FFR of Schnitzler et al. Core density would need to be decreased to allow the transport of the ffs out of the core, and a means of directing the ffs would still be required. If fission multiplication can be maintained with the lower density core, and the magnetic fields required to direct the ffs designed, significantly better rocket performance would be achieved.

V Summary

The antiproton-catalyzed fission fragment rocket ($\bar{p}$-FFR) was designed and modeled to assess its feasibility as a space propulsion system. While many assumptions were made in its development, an attempt was made to limit the advances in current technology required to construct the $\bar{p}$-FFR. The problem of $\bar{p}$ generation and storage remains unsolved, but other technologies used are within today's capabilities. With these facts in mind, the performance of the $\bar{p}$-FFR may be assessed.

Using a sub-critical FFR pile, the $\bar{p}$-U interaction can be made to generate amounts of usable energy equal to or greater than that available from the $\bar{p}$-p annihilation. Forward hypothesized that 35% of the $\bar{p}$ + p rest mass energy could be used for spacecraft propulsion. For an FFR with a fission fragment energy escape fraction of 0.5, a fission multiplication of 8 would produce comparable amounts of energy.

Calculations were accomplished to evaluate the fission multiplication and neutronics of an $\bar{p}$-FFR pile. These calculations showed that while using uranium enrichments of less than 25%, fission multiplications of greater than 8 could be achieved. This model pile also exhibited even neutron fluence distributions, which ensure an even burn-up. Neutron multiplication was seen to be less than 0.4 in the engines modeled, meeting the design goal of a sub-critical reactor.

In terms of rocket performance, the $\bar{p}$-FFR is limited by its unclad fuel assemblies. The rocket exhaust temperature is limited by the material characteristics of the fissile fuel coatings. For the UC coating

used, this limit is 2623 K. Rocket performance also suffers from the inability to use hydrogen as the exhaust gas. This limitation is due to the undesirable reaction of H and UC.

As was discussed in Section 4, many refinements are needed to completely characterize the performance of an $\bar{p}$-FFR. Treatment of the thermodynamics of the pile and exhaust gas needs to be more rigorous to fully evaluate this concept. An alternate method of thrust generation, exhausting the fission fragments themselves, would improve engine performance, if the technology exists to do this.

Based on the results seen here, the engine design presented is inadequate. The limitations introduced by the reaction fluid far outweigh the simplicity-of-design gained. Despite this, the basic idea of using the $\bar{p}$-U interaction as a source of spacecraft propulsion deserves further attention.

Appendix A MORSE Input Files and FORTRAN Codei

The following file was used to calculate fission multiplication. This file also contains the standard geometry input for Engine #2.

```
Fission Fragment Rocket UC sh=20  V=250
 1000 5000    5    1   46    0   46   46    0    0  200    3    0
    0   46    0    01.0         1.000E-5  0.          0.          4.384E3
       0.0         0.0   0341.4       0.0         0.0         0.0         0.0
 3.6090+00 2.7519-01 1.1120-01 6.3554-02 1.9292-01 1.2015-01 2.7219-01
 3.2145-01 3.4297-01 3.6154-01 3.9864-01 5.9771-01 1.1141+00 2.7990-01
 5.9722-01 1.2849+00 7.8155-01 1.3749-01 6.9171-01 5.3266-01 4.4436-01
 1.8859-01 1.8720-01 9.4483-02 1.2515-01 1.0800-01 1.9181-01 1.1688-01
 6.6370-02 3.1532-02 3.6108-02 4.3600-03 2.2900-03 7.7000-04 2.9200-03
 1.6200-03 5.4000-04 1.5300-04 7.5000-05 4.3200-05 1.7500-05 4.4000-06
 1.9000-06 4.9000-07 1.7000-07 1.0000-07
 1.9600 +7 1.6900 +7 1.4900 +7 1.4200 +7 1.3800 +7 1.2800 +7 1.2200 +7
 1.1100 +7 1.0000 +7 9.0000 +6 8.2000 +6 7.4000 +6 6.4000 +6 5.0000 +6
 4.7000 +6 4.1000 +6 3.0000 +6 2.4000 +6 2.3000 +6 1.8000 +6 1.4227 +6
 1.1000 +6 9.6164 +5 8.2085 +5 7.4274 +5 6.3928 +5 5.5000 +5 3.6883 +5
 2.4724 +5 1.6000 +5 1.1000 +5 5.2000 +4 3.4307 +4 2.5000 +4 2.1875 +4
 1.0000 +4 3.4000 +3 1.2000 +3 5.8000 +2 2.7536 +2 1.0000 +2 2.9000 +1
 1.1000 +1 3.1000 +0 1.1000 +0 4.1400 -1
45 FA231A
    0    1    0    0    0    2   46
    1    1   35    1    1    1    0.00 +0     0.1 +0     1.00+0     0.00 +0
   36    1   46    1    1    1    0.00 +0     0.5 -1     1.00+0     0.00 +0
    1    1   46    2    1    2    0.00 +0     0.1 +0     1.0 +0     0.00 +0
   -1
    0    1    1    0
 2.0000 -1 0.0000 +0 0.0000 +0 0.0000 +0
 0.0000 +0 0.0000 +0 0.0000 +0 0.0000 +0 0.0000 +0 1.3176 -7 2.8945 -4
 7.9429 -4 1.4732 -3 2.5439 -3 4.1137 -3 1.0382 -2 3.3574 -2 9.7134 -3
 3.5853 -2 1.0060 -1 9.8792 -2 1.5064 -2 1.0750 -1 1.0724 -1 1.0724 -1
 4.0544 -2 4.0544 -2 4.0544 -2 4.0544 -2 4.0544 -2 4.4188 -2 4.4188 -2
 4.4188 -2 1.1742 -2 1.1947 -2 2.0073 -3 2.0073 -3 3.3303 -4 1.0920 -3
 3.6106 -4 3.5729 -5 4.0425 -6 4.4773 -7 4.4773 -7 1.0950-11 0.0000 -0
 0.0000 -0 0.0000 -0 0.0000 -0 0.0000 -0
 0.0000 +0 0.0000 +0 0.0000 +0 0.0000 +0 0.0000 +0 0.0000 +0 0.0000 +0
 0.0000 +0 0.0000 +0 0.0000 +0 0.0000 +0 0.0000 +0 0.0000 +0 0.0000 +0
 0.0000 +0 0.0000 +0 0.0000 +0 0.0000 +0 0.0000 +0 0.0000 +0 0.0000 +0
 0.0000 +0 0.0000 +0 0.0000 +0 0.0000 +0 0.0000 +0 0.0000 +0 0.0000 +0
 0.0000 +0 0.0000 +0 0.0000 +0 0.0000 +0 0.0000 +0 0.0000 +0 0.0000 +0
 0.0000 +0 0.0000 +0 0.0000 +0 0.0000 +0 0.0000 +0 0.0000 +0 0.0000 +0
 0.0000 +0 0.0000 +0 0.0000 +0 0.0000 +0
 0.0000 +0 0.0000 +0 0.0000 +0 0.0000 +0 0.0000 +0 0.0000 +0 0.0000 +0
 0.0000 +0 0.0000 +0 0.0000 +0 0.0000 +0 0.0000 +0 0.0000 +0 0.0000 +0
```

```
0.0000 +0 0.0000 +0 0.0000 +0 0.0000 +0 0.0000 +0 0.0000 +0 0.0000 +0
0.0000 +0 0.0000 +0 0.0000 +0 0.0000 +0 0.0000 +0 0.0000 +0 0.0000 +0
0.0000 +0 0.0000 +0 0.0000 +0 0.0000 +0 0.0000 +0 0.0000 +0 0.0000 +0
0.0000 +0 0.0000 +0 0.0000 +0 0.0000 +0 0.0000 +0 0.0000 +0 0.0000 +0
0.0000 +0 0.0000 +0 0.0000 +0 0.0000 +0
3     0                          COMBINATORIAL GEOM  FFR U-fiber Pile
 RCC     0          0          000.0     0          0          6.8278+2
         3.41392 +2
 RCC     0          0          -20.0     0          0          7.2278+2
         3.61392 +2
 RCC     0          0          -100.0    0          0          1.0   +2
         25.000  +0
 RCC     0          0          -22.0     0          0          7.2678+2
         3.63392 +2
 RCC     0          0          -1.0+3    0          0          3.0   +3
         3.0000  +3
 END
   1           +1
   2           +2      -1      -3
   3           +4      -2      -3
   4           +5      -4
   5           +3
 END
   1    2    2    2    2
   1    2    3    0 1000
2.5000+8  4.6582+7  2.1206+10
46 G N CROSS SECTIONS (DABL69) -- P3--
   46   46    0    0   69   72    4    3    5    6    4    2    1    3
    0    0    0    0    0    0    0  -10    0    0    0
SAMBO ANALYSIS INPUT DATA FOR FFR PROBLEM
    2    2    2    0    0    2    1    1
       0.0       0.0       0.0
       0.0       0.0       0.0
FFR U-Pille Neutron Detectors
{fissions/source neutron}
0.1979    0.2117    0.2206    0.2247    0.2305    0.2378    0.2466
0.2563    0.2631    0.2696    0.2773    0.2896    0.3120    0.3265
0.3350    0.3508    0.3645    0.3702    0.3749    0.3857    0.3860
0.3975    0.3975    0.3975    0.3975    0.3975    0.4071    0.4071
0.4071    0.4105    0.4116    0.4125    0.4125    0.4128    0.4129
0.4131    0.4132    0.4132    0.4132    0.4132    0.4132    0.4132
0.4132    0.4132    0.4132    0.4132
{absorptions/source neutron}
1.0000    1.0000    1.0000    1.0000    1.0000    1.0000    1.0000
1.0000    1.0000    1.0000    1.0000    1.0000    1.0000    1.0000
1.0000    1.0000    1.0000    1.0000    1.0000    1.0000    1.0000
1.0000    1.0000    1.0000    1.0000    1.0000    1.0000    1.0000
1.0000    1.0000    1.0000    1.0000    1.0000    1.0000    1.0000
1.0000    1.0000    1.0000    1.0000    1.0000    1.0000    1.0000
1.0000    1.0000    1.0000    1.0000
```

```
(neutrons/cm^2)
   46   46
$$$$$$$$ FFR U-fiber Pile HIDINGER 25 Oct 91  $$$$$$$$
```

The following input file was used to calculate k_{eff}. This file also contains the standard geometery input for Engine #1.

```
Fission Fragment Rocket UC sh=20 V=125 Keff Calc
 010010000    14     1    46     0    46    46     0     0  800     3     0
     0   46     0     01.0        1.000E-5  0.         0.          4.384E3
        0.0         0.0   0341.4        0.0         0.0        0.0        0.0
 3.6090+00 2.7519-01 1.1120-01 6.3554-02 1.9292-01 1.2015-01 2.7219-01
 3.2145-01 3.4297-01 3.6154-01 3.9864-01 5.9771-01 1.1141+00 2.7990-01
 5.9722-01 1.2849+00 7.8155-01 1.3749-01 6.9171-01 5.3266-01 4.4436-01
 1.8859-01 1.8720-01 9.4483-02 1.2515-01 1.0800-01 1.9181-01 1.1688-01
 6.6370-02 3.1532-02 3.6108-02 4.3600-03 2.2900-03 7.7000-04 2.9200-03
 1.6200-03 5.4000-04 1.5300-04 7.5000-05 4.3200-05 1.7500-05 4.4000-06
 1.9000-06 4.9000-07 1.7000-07 1.0000-07
 1.9600 +7 1.6900 +7 1.4900 +7 1.4200 +7 1.3800 +7 1.2800 +7 1.2200 +7
 1.1100 +7 1.0000 +7 9.0000 +6 8.2000 +6 7.4000 +6 6.4000 +6 5.0000 +6
 4.7000 +6 4.1000 +6 3.0000 +6 2.4000 +6 2.3000 +6 1.8000 +6 1.4227 +6
 1.1000 +6 9.6164 +5 8.2085 +5 7.4274 +5 6.3928 +5 5.5000 +5 3.6883 +5
 2.4724 +5 1.6000 +5 1.1000 +5 5.2000 +4 3.4307 +4 2.5000 +4 2.1875 +4
 1.0000 +4 3.4000 +3 1.2000 +3 5.8000 +2 2.7536 +2 1.0000 +2 2.9000 +1
 1.1000 +1 3.1000 +0 1.1000 +0 4.1400 -1
45 FA231A
    0    1     0     0     0     2    46
    1    1    35     1     1     1    0.00 +0     0.1 +0     1.00+0    0.00 +0
   36    1    46     1     1     1    0.00 +0     0.5 -1     1.00+0    0.00 +0
    1    1    46     2     1     2    0.00 +0     0.1 +0     1.0 +0    0.00 +0
   -1
    1    1     4     1
 2.0000 -1 0.0000 +0 0.0000 +0 0.0000 +0
 0.0000 +0 0.0000 +0 0.0000 +0 0.0000 +0 0.0000 +0 1.3176 -7 2.8945 -4
 7.9429 -4 1.4732 -3 2.5439 -3 4.1137 -3 1.0382 -2 3.3574 -2 9.7134 -3
 3.5853 -2 1.0060 -1 9.8792 -2 1.5064 -2 1.0750 -1 1.0724 -1 1.0724 -1
 4.0544 -2 4.0544 -2 4.0544 -2 4.0544 -2 4.0544 -2 4.4188 -2 4.4188 -2
 4.4188 -2 1.1742 -2 1.1947 -2 2.0073 -3 2.0073 -3 3.3303 -4 1.0920 -3
 3.6106 -4 3.5729 -5 4.0425 -6 4.4773 -7 4.4773 -7 1.0950-11 0.0000 -0
 0.0000 -0 0.0000 -0 0.0000 -0 0.0000 -0
 0.0000 +0 0.0000 +0 0.0000 +0 0.0000 +0 0.0000 +0 0.0000 +0 0.0000 +0
 0.0000 +0 0.0000 +0 0.0000 +0 0.0000 +0 0.0000 +0 0.0000 +0 0.0000 +0
 0.0000 +0 0.0000 +0 0.0000 +0 0.0000 +0 0.0000 +0 0.0000 +0 0.0000 +0
 0.0000 +0 0.0000 +0 0.0000 +0 0.0000 +0 0.0000 +0 0.0000 +0 0.0000 +0
 0.0000 +0 0.0000 +0 0.0000 +0 0.0000 +0 0.0000 +0 0.0000 +0 0.0000 +0
 0.0000 +0 0.0000 +0 0.0000 +0 0.0000 +0 0.0000 +0 0.0000 +0 0.0000 +0
 0.0000 +0 0.0000 +0 0.0000 +0 0.0000 +0
 0.0000 +0 0.0000 +0 0.0000 +0 0.0000 +0 0.0000 +0 0.0000 +0 0.0000 +0
```

```
0.0000 +0 0.0000 +0 0.0000 +0 0.0000 +0 0.0000 +0 0.0000 +0 0.0000 +0
0.0000 +0 0.0000 +0 0.0000 +0 0.0000 +0 0.0000 +0 0.0000 +0 0.0000 +0
0.0000 +0 0.0000 +0 0.0000 +0 0.0000 +0 0.0000 +0 0.0000 +0 0.0000 +0
0.0000 +0 0.0000 +0 0.0000 +0 0.0000 +0 0.0000 +0 0.0000 +0 0.0000 +0
0.0000 +0 0.0000 +0 0.0000 +0 0.0000 +0 0.0000 +0 0.0000 +0 0.0000 +0
0.0000 +0 0.0000 +0 0.0000 +0 0.0000 +0
3     0                          COMBINATORIAL GEOM  FFR U-fiber Pile
 RCC      0          0          000.0      0          0          5.4193+2
          2.70965 +2
 RCC      0          0          -20.0      0          0          5.8193+2
          2.90965 +2
 RCC      0          0          -100.0     0          0          1.0   +2
          25.000  +0
 RCC      0          0          -22.0      0          0          5.8593+2
          2.92965 +2
 RCC      0          0          -1.0+3     0          0          3.0   +3
          3.0000  +3
 END
   1           +1
   2           +2      -1      -3
   3           +4      -2      -3
   4           +5      -4
   5           +3
 END
   1    2    2    2    2
   1    2    3    0 1000
2.5000+8  4.6582+7  2.1206+10
46 G N CROSS SECTIONS (DABL69) -- P3--
   46   46    0    0   69   72    4    3    5    6    4    2    1    3
    0    0    0    0    0    0    0  -10    0    0    0
SAMBO ANALYSIS INPUT DATA FOR FFR PROBLEM
    2    2    2    0    0    2    1    1
       0.0       0.0       0.0
       0.0       0.0       0.0
FFR U-Pille Neutron Detectors
{fissions/source neutron}
0.1979    0.2117    0.2206    0.2247    0.2305    0.2378    0.2466
0.2563    0.2631    0.2696    0.2773    0.2896    0.3120    0.3265
0.3350    0.3508    0.3645    0.3702    0.3749    0.3857    0.3860
0.3975    0.3975    0.3975    0.3975    0.3975    0.4071    0.4071
0.4071    0.4105    0.4116    0.4125    0.4125    0.4128    0.4129
0.4131    0.4132    0.4132    0.4132    0.4132    0.4132    0.4132
0.4132    0.4132    0.4132    0.4132
{absorptions/source neutron}
1.0000    1.0000    1.0000    1.0000    1.0000    1.0000    1.0000
1.0000    1.0000    1.0000    1.0000    1.0000    1.0000    1.0000
1.0000    1.0000    1.0000    1.0000    1.0000    1.0000    1.0000
1.0000    1.0000    1.0000    1.0000    1.0000    1.0000    1.0000
1.0000    1.0000    1.0000    1.0000    1.0000    1.0000    1.0000
1.0000    1.0000    1.0000    1.0000    1.0000    1.0000    1.0000
```

```
1.0000    1.0000    1.0000    1.0000
(neutrons/cm^2)
   46   46
$$$$$$$$ FFR U-fiber Pile HIDINGER 25 Oct 91  $$$$$$$$
```

The following input file was used to calculate radial fluence in Engine #1.

```
Fission Fragment Rocket UC sh=20  V=250 Radial Fluence Calc
 1000 5000   05    1   46    0   46   46    0    0 1000    3    0
    0   46    0    01.0        1.000E-5  0.        0.        4.384E3
       0.0       0.0   0341.4       0.0       0.0       0.0       0.0
 3.6090+00 2.7519-01 1.1120-01 6.3554-02 1.9292-01 1.2015-01 2.7219-01
 3.2145-01 3.4297-01 3.6154-01 3.9864-01 5.9771-01 1.1141+00 2.7990-01
 5.9722-01 1.2849+00 7.8155-01 1.3749-01 6.9171-01 5.3266-01 4.4436-01
 1.8859-01 1.8720-01 9.4483-02 1.2515-01 1.0800-01 1.9181-01 1.1688-01
 6.6370-02 3.1532-02 3.6108-02 4.3600-03 2.2900-03 7.7000-04 2.9200-03
 1.6200-03 5.4000-04 1.5300-04 7.5000-05 4.3200-05 1.7500-05 4.4000-06
 1.9000-06 4.9000-07 1.7000-07 1.0000-07
 1.9600 +7 1.6900 +7 1.4900 +7 1.4200 +7 1.3800 +7 1.2800 +7 1.2200 +7
 1.1100 +7 1.0000 +7 9.0000 +6 8.2000 +6 7.4000 +6 6.4000 +6 5.0000 +6
 4.7000 +6 4.1000 +6 3.0000 +6 2.4000 +6 2.3000 +6 1.8000 +6 1.4227 +6
 1.1000 +6 9.6164 +5 8.2085 +5 7.4274 +5 6.3928 +5 5.5000 +5 3.6883 +5
 2.4724 +5 1.6000 +5 1.1000 +5 5.2000 +4 3.4307 +4 2.5000 +4 2.1875 +4
 1.0000 +4 3.4000 +3 1.2000 +3 5.8000 +2 2.7536 +2 1.0000 +2 2.9000 +1
 1.1000 +1 3.1000 +0 1.1000 +0 4.1400 -1
45 PA231A
    0    1    0    0    0    2   46
    1    1   35    1    1    1   0.00 +0    0.1 +0    1.00+0    0.00 +0
   36    1   46    1    1    1   0.00 +0    0.5 -1    1.00+0    0.00 +0
    1    1   46    2    1    2   0.00 +0    0.1 +0    1.0 +0    0.00 +0
   -1
    0    1    1    0
 2.0000 -1 0.0000 +0 0.0000 +0 0.0000 +0
 0.0000 +0 0.0000 +0 0.0000 +0 0.0000 +0 0.0000 +0 1.3176 -7 2.8945 -4
 7.9429 -4 1.4732 -3 2.5439 -3 4.1137 -3 1.0382 -2 3.3574 -2 9.7134 -3
 3.5853 -2 1.0060 -1 9.8792 -2 1.5064 -2 1.0750 -1 1.0724 -1 1.0724 -1
 4.0544 -2 4.0544 -2 4.0544 -2 4.0544 -2 4.0544 -2 4.4188 -2 4.4188 -2
 4.4188 -2 1.1742 -2 1.1947 -2 2.0073 -3 2.0073 -3 3.3303 -4 1.0920 -3
 3.6106 -4 3.5729 -5 4.0425 -6 4.4773 -7 4.4773 -7 1.0950-11 0.0000 -0
 0.0000 -0 0.0000 -0 0.0000 -0 0.0000 -0
 0.0000 +0 0.0000 +0 0.0000 +0 0.0000 +0 0.0000 +0 0.0000 +0 0.0000 +0
 0.0000 +0 0.0000 +0 0.0000 +0 0.0000 +0 0.0000 +0 0.0000 +0 0.0000 +0
 0.0000 +0 0.0000 +0 0.0000 +0 0.0000 +0 0.0000 +0 0.0000 +0 0.0000 +0
 0.0000 +0 0.0000 +0 0.0000 +0 0.0000 +0 0.0000 +0 0.0000 +0 0.0000 +0
 0.0000 +0 0.0000 +0 0.0000 +0 0.0000 +0 0.0000 +0 0.0000 +0 0.0000 +0
 0.0000 +0 0.0000 +0 0.0000 +0 0.0000 +0
```

```
0.0000 +0 0.0000 +0 0.0000 +0 0.0000 +0 0.0000 +0 0.0000 +0 0.0000 +0
0.0000 +0 0.0000 +0 0.0000 +0 0.0000 +0 0.0000 +0 0.0000 +0 0.0000 +0
0.0000 +0 0.0000 +0 0.0000 +0 0.0000 +0 0.0000 +0 0.0000 +0 0.0000 +0
0.0000 +0 0.0000 +0 0.0000 +0 0.0000 +0 0.0000 +0 0.0000 +0 0.0000 +0
0.0000 +0 0.0000 +0 0.0000 +0 0.0000 +0 0.0000 +0 0.0000 +0 0.0000 +0
0.0000 +0 0.0000 +0 0.0000 +0 0.0000 +0 0.0000 +0 0.0000 +0 0.0000 +0
0.0000 +0 0.0000 +0 0.0000 +0 0.0000 +0
3     0                          COMBINATORIAL GEOM  FFR U-fiber Pile
 RCC      0         0          000.0     0         0         5.4193+2
          0.85688 +2
 RCC      0         0          000.0     0         0         5.4193+2
          1.21178 +2
 RCC      0         0          000.0     0         0         5.4193+2
          1.48412 +2
 RCC      0         0            0       0         0         5.4193+2
          1.71371 +2
 RCC      0         0            0       0         0         5.4193+2
          1.91599 +2
 RCC      0         0            0       0         0         5.4193+2
          2.09886 +2
 RCC      0         0            0       0         0         5.4193+2
          2.26703+2
 RCC      0         0            0       0         0         5.4193+2
          2.42356+2
 RCC      0         0            0       0         0         5.4193+2
          2.57057+2
 RCC      0         0            0       0         0         5.4193 +2
          2.70965+2
 RCC      0         0          -20.0     0         0         5.8193+2
          2.90965 +2
 RCC      0         0          -100.0    0         0         1.0    +2
          25.000  +0
 RCC      0         0          -22.0     0         0         5.8593+2
          2.92965 +2
 RCC      0         0          -1.0+3    0         0         3.0    +3
          3.0000  +3
 END
   1          +1
   2          +2      -1
   3          +3      -2
   4          +4      -3
   5          +5      -4
   6          +6      -5
   7          +7      -6
   8          +8      -7
   9          +9      -8
  10          +10     -9
  11          +11     -10     -12
  12          +13     -11     -12
  13          +14     -13
```

```
  14          +12
 END
   1    1    1    1    1    1    1    1    1    1    2    2    2    2
   1    1    1    1    1    1    1    1    1    1    2    3    0 1000
2.5000+8  2.5000+8  2.5000+8  2.5000+8   2.5000+8 2.5000+8   2.5000+8
46 G N CROSS SECTIONS (DABL69) -- P3--
  46   46    0    0   69   72    4    3    5    6    4    2    1    3
   0    0    0    0    0    0    0  -10    0    0    0
SAMBO ANALYSIS INPUT DATA FOR FFR PROBLEM
  10    1    1    0    0    1    1    1
      0.0       0.0       0.0
      0.0       0.0       0.0
      0.0       0.0       0.0
      0.0       0.0       0.0
      0.0       0.0       0.0
      0.0       0.0       0.0
      0.0       0.0       0.0
      0.0       0.0       0.0
      0.0       0.0       0.0
      0.0       0.0       0.0
FFR U-Pille Neutron Detectors
{Path Length Accumulator}
1.0000    1.0000    1.0000    1.0000    1.0000    1.0000    1.0000
1.0000    1.0000    1.0000    1.0000    1.0000    1.0000    1.0000
1.0000    1.0000    1.0000    1.0000    1.0000    1.0000    1.0000
1.0000    1.0000    1.0000    1.0000    1.0000    1.0000    1.0000
1.0000    1.0000    1.0000    1.0000    1.0000    1.0000    1.0000
1.0000    1.0000    1.0000    1.0000    1.0000    1.0000    1.0000
1.0000    1.0000    1.0000    1.0000
$$$$$$$$ FFR U-fiber Pile HIDINGER 25 Oct 91  $$$$$$$$
```

The following input file was used to calculate axial fluence.

```
Fission Fragment Rocket UC sh=20  V=250 Axial Fluence Calc
 1000 5000   05    1   46    0   46   46    0    0 1000    3    0
    0   46    0   01.0       1.000E-5  0.        0.        4.384E3
      0.0       0.0   0341.4       0.0       0.0       0.0       0.0
 3.6090+00 2.7519-01 1.1120-01 6.3554-02 1.9292-01 1.2015-01 2.7219-01
 3.2145-01 3.4297-01 3.6154-01 3.9864-01 5.9771-01 1.1141+00 2.7990-01
 5.9722-01 1.2849+00 7.8155-01 1.3749-01 6.9171-01 5.3266-01 4.4436-01
 1.8859-01 1.8720-01 9.4483-02 1.2515-01 1.0800-01 1.9181-01 1.1688-01
 6.6370-02 3.1532-02 3.6108-02 4.3600-03 2.2900-03 7.7000-04 2.9200-03
 1.6200-03 5.4000-04 1.5300-04 7.5000-05 4.3200-05 1.7500-05 4.4000-06
 1.9000-06 4.9000-07 1.7000-07 1.0000-07
 1.9600 +7 1.6900 +7 1.4900 +7 1.4200 +7 1.3800 +7 1.2800 +7 1.2200 +7
 1.1100 +7 1.0000 +7 9.0000 +6 8.2000 +6 7.4000 +6 6.4000 +6 5.0000 +6
 4.7000 +6 4.1000 +6 3.0000 +6 2.4000 +6 2.3000 +6 1.8000 +6 1.4227 +6
 1.1000 +6 9.6164 +5 8.2085 +5 7.4274 +5 6.3928 +5 5.5000 +5 3.6883 +5
 2.4724 +5 1.6000 +5 1.1000 +5 5.2000 +4 3.4307 +4 2.5000 +4 2.1875 +4
```

```
 1.0000 +4 3.4000 +3 1.2000 +3 5.8000 +2 2.7536 +2 1.0000 -2 2.9000 +1
 1.1000 +1 3.1000 +0 1.1000 +0 4.1400 -1
45 FA231A
    0    1    0    0    0    2    46
    1    1   35    1    1    1    0.00 +0      0.1 +0      1.00+0     0.00 +0
   36    1   46    1    1    1    0.00 +0      0.5 -1      1.00+0     0.00 +0
    1    1   46    2    1    2    0.00 +0      0.1 +0      1.0 +0     0.00 +0
   -1
    0    1    1    0
 2.0000 -1 0.0000 +0 0.0000 +0 0.0000 +0
 0.0000 +0 0.0000 +0 0.0000 +0 0.0000 +0 0.0000 +0 1.3176 -7 2.8945 -4
 7.9429 -4 1.4732 -3 2.5439 -3 4.1137 -3 1.0382 -2 3.3574 -2 9.7134 -3
 3.5853 -2 1.0060 -1 9.8792 -2 1.5064 -2 1.0750 -1 1.0724 -1 1.0724 -1
 4.0544 -2 4.0544 -2 4.0544 -2 4.0544 -2 4.0544 -2 4.4188 -2 4.4188 -2
 4.4188 -2 1.1742 -2 1.1947 -2 2.0073 -3 2.0073 -3 3.3303 -4 1.0920 -3
 3.6106 -4 3.5729 -5 4.0425 -6 4.4773 -7 4.4773 -7 1.0950-11 0.0000 -0
 0.0000 -0 0.0000 -0 0.0000 -0 0.0000 -0
 0.0000 +0 0.0000 +0 0.0000 +0 0.0000 +0 0.0000 +0 0.0000 +0 0.0000 +0
 0.0000 +0 0.0000 +0 0.0000 +0 0.0000 +0 0.0000 +0 0.0000 +0 0.0000 +0
 0.0000 +0 0.0000 +0 0.0000 +0 0.0000 +0 0.0000 +0 0.0000 +0 0.0000 +0
 0.0000 +0 0.0000 +0 0.0000 +0 0.0000 +0 0.0000 +0 0.0000 +0 0.0000 +0
 0.0000 +0 0.0000 +0 0.0000 +0 0.0000 +0 0.0000 +0 0.0000 +0 0.0000 +0
 0.0000 +0 0.0000 +0 0.0000 +0 0.0000 +0 0.0000 +0 0.0000 +0 0.0000 +0
 0.0000 +0 0.0000 +0 0.0000 +0 0.0000 +0
 0.0000 +0 0.0000 +0 0.0000 +0 0.0000 +0 0.0000 +0 0.0000 +0 0.0000 +0
 0.0000 +0 0.0000 +0 0.0000 +0 0.0000 +0 0.0000 +0 0.0000 +0 0.0000 +0
 0.0000 +0 0.0000 +0 0.0000 +0 0.0000 +0 0.0000 +0 0.0000 +0 0.0000 +0
 0.0000 +0 0.0000 +0 0.0000 +0 0.0000 +0 0.0000 +0 0.0000 +0 0.0000 +0
 0.0000 +0 0.0000 +0 0.0000 +0 0.0000 +0 0.0000 +0 0.0000 +0 0.0000 +0
 0.0000 +0 0.0000 +0 0.0000 +0 0.0000 +0 0.0000 +0 0.0000 +0 0.0000 +0
 0.0000 +0 0.0000 +0 0.0000 +0 0.0000 +0
 3     0                                 COMBINATORIAL GEOM  FFR U-fiber Pile
  RCC       0          0            0.0       0         0           5.4193+1
            2.70965 +2
  RCC       0          0            0.0       0         0           1.08386+2
            2.70965 +2
  RCC       0          0            0.0       0         0           1.62579+2
            2.70965 +2
  RCC       0          0            0.0       0         0           2.16772+2
            2.70965 +2
  RCC       0          0            0.0       0         0           2.70965+2
            2.70965 +2
  RCC       0          0            0.0       0         0           3.25158+2
            2.70965 +2
  RCC       0          0            0.0       0         0           3.79351+2
            2.70965+2
  RCC       0          0            0.0       0         0           4.33544+2
            2.70965+2
  RCC       0          0            0.0       0         0           4.87737+2
            2.70965+2
```

```
  RCC     0          0          0.0       0          0          5.4193+2
          2.70965+2
  RCC     0          0          -20.0     0          0          5.8193+2
          2.90965 +2
  RCC     0          0          -100.0    0          0          1.0   +2
          25.000  +0
  RCC     0          0          -22.0     0          0          5.8593+2
          2.92965 +2
  RCC     0          0          -1.0+3    0          0          3.0   +3
          3.0000  +3
  END
    1          +1
    2          +2       -1
    3          +3       -2
    4          +4       -3
    5          +5       -4
    6          +6       -5
    7          +7       -6
    8          +8       -7
    9          +9       -8
   10          +10      -9
   11          +11      -10      -12
   12          +13      -11      -12
   13          +14      -13
   14          +12
  END
    1    1    1    1    1    1    1    1    1    1    2    2    2    2
    1    1    1    1    1    1    1    1    1    1    2    3    0 1000
2.5000+8  2.5000+8  2.5000+8  2.5000+8  2.5000+8 2.5000+8  2.5000+8
46 G N CROSS SECTIONS (DABL69) -- P3--
   46   46    0    0   69   72    4    3    5    6    4    2    1    3
    0    0    0    0    0    0    0  -10    0    0    0
SAMBO ANALYSIS INPUT DATA FOR FFR PROBLEM
   10    1    1    0    0    1    1    1
       0.0       0.0       0.0
       0.0       0.0       0.0
       0.0       0.0       0.0
       0.0       0.0       0.0
       0.0       0.0       0.0
       0.0       0.0       0.0
       0.0       0.0       0.0
       0.0       0.0       0.0
       0.0       0.0       0.0
       0.0       0.0       0.0
FFR U-Pille Neutron Detectors
{Path Length Accumulator}
1.0000    1.0000    1.0000    1.0000    1.0000    1.0000    1.0000
1.0000    1.0000    1.0000    1.0000    1.0000    1.0000    1.0000
1.0000    1.0000    1.0000    1.0000    1.0000    1.0000    1.0000
1.0000    1.0000    1.0000    1.0000    1.0000    1.0000    1.0000
```

```
1.0000    1.0000    1.0000    1.0000    1.0000    1.0000    1.0000
1.0000    1.0000    1.0000    1.0000    1.0000    1.0000    1.0000
1.0000    1.0000    1.0000    1.0000
$$$$$$$$ FFR U-fiber Pile HIDINGER 25 Oct 91  $$$$$$$$
```

The following FORTRAN code was used in calculating the radial fluence :

```
C      RADIALFLUX.FOR  (20125 FFR Configuration)
C*********************************************************************
C*        This version does not determine uncollided fluence.        *
C*        Instead, a tracklength estimater is used to determine      *
C*        fluence and is called for collisions and boundary crossings. *
C*********************************************************************
C * * THIS IS THE MAIN ROUTINE * * * * * * * * * * * * * * * * * * * *
C * * D. HIDINGER, Oct 91, FFR U-pile 1 region,  10 detectors
C * * THE POLLOWING CARD DETERMINES THE SIZE ALLOWED FOR BLANK COMMON  *
c * * The value of NLFT below should be set to one less than this size
      COMMON NC(700000)
C * *  (REGION SIZE NEEDED IS ABOUT 150K + 4*(SIZE OF BLANK COMMON IN WO
C * * NOTE - THE ORDER OF COMMONS IN THIS ROUTINE IS IMPORTANT AND MUST
C * *   POND TO THE ORDER USED IN DUMP ROUTINES SUCH AS HELP, XSCHLP, AN
C * *
C * * LABELLED COMMONS FOR WALK ROUTINES    * * * * * * * * * * * * * * *
      COMMON /APOLLO/ AGSTRT,DDF,DEADWT(26),ITOUT,ITIN
      COMMON /FISBNK/ MFISTP
      COMMON /NUTRON/ NAME
C * *
C * * LABELLED COMMONS FOR CROSS-SECTION ROUTINES  * * * * * * * * * * * *
      COMMON /LOCSIG/ ISCCOG
      COMMON /MEANS/ NM
      COMMON /MOMENT/ NMOM
      COMMON /QAL/ Q
      COMMON /RESULT/ POINT
C * *
C * * LABELLED COMMONS FOR GEOMETRY INTERFACE ROUTINES  * * * * * * * *
      COMMON /GEOMC/ XTWO
      COMMON /NORMAL/ UNORM
C * *
C * * LABELLED COMMONS FOR USER ROUTINES  * * * * * * * * * * * * * * * *
      COMMON /PDET/ ND
      COMMON /USER/ AGST
C * *
C * * COMMON /DUMMY/ WILL NOT BE FOUND ELSEWHERE IN THE PROGRAM  * * * *
      COMMON /DUMMY/ DUM
C * *
        CHARACTER*40, NAM1
        CHARACTER*40, NAM2
```

```
        TYPE *,' '
        TYPE *,'********* MORSE Code, FFR Problem *********'
        TYPE *,'========> WARNING !!! <========'
        TYPE *,'ABORT if mixed x-secs are not assigned to FOR010'
        TYPE *,' '
        TYPE *,'ENTER NAME OF INPUT FILE'
        ACCEPT 100, NAM1
100     FORMAT(A40)
        TYPE *,'ENTER NAME OF OUTPUT FILE'
        ACCEPT 200, NAM2
200     FORMAT (A40)
        OPEN(UNIT=1,NAME=NAM1,TYPE='OLD')
        OPEN(UNIT=2,NAME=NAM2,TYPE='NEW')
      ITOUT = 2
      ITIN = 1
        NLFT=699999
      CALL MORSE(NLFT)
        TYPE 300, NAM2
300     FORMAT(X,'OUTPUT FILE IS ',A40)
      STOP
      END
      SUBROUTINE GTMED(MDGEOM,MDXSEC)
c   this version for two region FFR pile 1 = fissile, 2 = reflector
      MDXSEC = MDGEOM
      RETURN
      END
      FUNCTION DIREC(F)
      direc=1.
C
      RETURN
      END
      SUBROUTINE BANKR(NBNKID)
C  DO NOT CALL EUCLID FROM BANKR(7)
      COMMON /APOLLO/ AGSTRT,DDF,DEADWT(5),ETA,ETATH,ETAUSD,UINP,VINP,
     1 WINP,WTSTRT,XSTRT,YSTRT,ZSTRT,TCUT,XTRA(10),
     2   IO,I1,MEDIA,IADJM,ISBIAS,ISOUR,ITERS,ITIME,ITSTR,LOCWTS,LOCFWL,
     3 LOCEPR,LOCNSC,LOCFSN,MAXGP,MAXTIM,MEDALB,MGPREG,MXREG,NALB,
     4 NDEAD(5),NEWNM,NGEOM,NGPQT1,NGPQT2,NGPQT3,NGPQTG,NGPQTN,NITS,
     5 NKCALC,NKILL,NLAST,NMEM,NMGP,NMOST,NMTG,NOLEAK,NORMF,NPAST,
     6 NPSCL(13),NQUIT,NSIGL,NSOUR,NSPLT,NSTRT,NXTRA(10)
      COMMON /NUTRON/ NAME,NAMEX,IG,IGO,NMED,MEDOLD,NREG,U,V,W,UOLD,VOLD
     1 ,WOLD,X,Y,Z,XOLD,YOLD,ZOLD,WATE,OLDWT,WTBC,BLZNT,BLZON,AGE,OLDAGE
      NBNK = NBNKID
      IF (NBNK) 100,100,140
  100 NBNK = NBNK + 5
      GO TO (104,103,102,101),NBNK
  101 CALL STRUN
C     CALL HELP(4HSTRU,1,1,1,1)
      RETURN
  102 NBAT = NITS - ITERS
```

```
      NSAVE = NMEM
      CALL STBTCH(NBAT)
C   NBAT IS THE BATCH NO. LESS ONE
      RETURN
  103 CALL NBATCH(NSAVE)
C   NSAVE IS THE NO. OF PARTICLES STARTED IN THE LAST BATCH
      RETURN
  104 CALL NRUN(NITS,NQUIT)
C   NITS IS THE NO. OF BATCHES COMPLETED IN THE RUN JUST COMPLETED
C   NQUIT .GT. 1 IF MORE RUNS REMAIN
C         .EQ. 1 IF THE LAST SCHEDULED RUN HAS BEEN COMPLETED
C         IS THE NEGATIVE OF THE NO. OF COMPLETE RUNS, WHEN AN
C              EXECUTION TIME KILL OCCURS
      RETURN
  140 GO TO (1,2,3,4,5,6,7,8,9,10,11,12,13),NBNK
C  NBNKID   COLL TYPE   BANKR CALL      NBNKID   COLL TYPE   BANKR CALL
C     1      SOURCE     YES (MSOUR)       2      SPLIT      NO  (TESTW)
C     3      FISSION    YES (FPROB)       4      GAMGEN     YES (GSTORE
C     5      REAL COLL  YES (MORSE)       6      ALBEDO     YES (MORSE)
C     7      BDRYX      YES (NXTCOL)      8      ESCAPE     YES (NXTCOL
C     9      E-CUT      NO  (MORSE)      10      TIME KILL  NO  (MORSE)
C    11      R R KILL   NO  (TESTW)      12      R R SURV   NO  (TESTW)
C    13      GAMLOST    NO  (GSTORE)
    1 RETURN
    2 RETURN
    3 RETURN
    4 RETURN
    5 CALL TRKCOL
      RETURN
    6 RETURN
    7 CALL TRKBDR
      RETURN
    8 RETURN
    9 RETURN
   10 RETURN
   11 RETURN
   12 RETURN
   13 RETURN
      END
      SUBROUTINE TRKBDR
C*********************************************************************
C   this version sums track length for fluence
C
C       MEDIA:  1   - fissile fiber pile
C               2   - reflector
C               3  - AL Shell
C            1000 - Interior void
C               0 - Exterior void
C*********************************************************************
      COMMON /PDET/ ND,NNE,NE,NT,NA,NRESP,NEX,NEXND,NEND,NDNR,NTNR,NTNE,
```

```
     1 NANE,NTNDNR,NTNEND,NANEND,LOCRSP,LOCXD,LOCIB,LOCCO,LOCT,LOCUD,
     2 LOCSD,LOCQE,LOCQT,LOCQTE,LOCQAE,LMAX,EFIRST,EGTOP
      COMMON /NUTRON/ NAME,NAMEX,IG,IGO,NMED,MEDOLD,NREG,U,V,W,UOLD,VOLD
     1 ,WOLD,X,Y,Z,XOLD,YOLD,ZOLD,WATE,OLDWT,WTBC,BLZNT,BLZON,AGE,OLDAGE
C * * * check for neutron not coming from fission region  * * *
      IF(MEDOLD.ne.1)RETURN
C * * * add track length to zone detector * * *
      TRK = WATE * SQRT((X-XOLD)**2 + (Y-YOLD)**2 + (Z-ZOLD)**2)
c  * * *  determine which shell, direction and detector
      RAD = SQRT(X**2 + Y**2)
      OLDRAD=SQRT(XOLD**2 +YOLD**2)
      delrad=RAD-OLDRAD
c  * * * Check for particle passing shell to shell
      if(nmed.ne.1) delrad=1
      rad1=85.688
      rad2=121.178
      rad3=148.412
      rad4=171.371
      rad5=191.599
      rad6=209.886
      rad7=226.703
      rad8=242.356
      rad9=257.057
      rad10=270.965
      if(RAD.le.rad1) ndetec = 1
      if((RAD.le.rad2).and.(RAD.gt.rad1)) ndetec=2
      if((RAD.le.rad3).and.(RAD.gt.rad2)) ndetec=3
      if((RAD.le.rad4).and.(RAD.gt.rad3)) ndetec=4
      if((RAD.le.rad5).and.(RAD.gt.rad4)) ndetec=5
      if((RAD.le.rad6).and.(RAD.gt.rad5)) ndetec=6
      if((RAD.le.rad7).and.(RAD.gt.rad6)) ndetec=7
      if((RAD.le.rad8).and.(RAD.gt.rad7)) ndetec=8
      if((RAD.le.rad9).and.(RAD.gt.rad8)) ndetec=9
      if((RAD.le.rad10).and.(RAD.gt.rad9)) ndetec=10
      if (delrad.lt.0) ndetec = ndetec + 1
      CON = TRK
      goto 101

  101 CALL FLUXST(NDETEC,IG,CON,0.0,0.0,0)
C  *  *  SWITCH =  0  -- STORE IN ALL RELEVANT ARRAYS EXCEPT UD
      RETURN
      END
      SUBROUTINE TRKCOL
C**********************************************************************
C   this version determines flux from tracklength divided by detector
C   volume and is used with TRKBDR (called from BANKR(7))
C**********************************************************************
      COMMON /PDET/ ND,NNE,NE,NT,NA,NRESP,NEX,NEXND,NEND,NDNR,NTNR,NTNE,
     1 NANE,NTNDNR,NTNEND,NANEND,LOCRSP,LOCXD,LOCIB,LOCCO,LOCT,LOCUD,
     2 LOCSD,LOCQE,LOCQT,LOCQTE,LOCQAE,LMAX,EFIRST,EGTOP
```

```
      COMMON /NUTRON/ NAME,NAMEX,IG,IGO,NMED,MEDOLD,NREG,U,V,W,UOLD,VOLD
     1 ,WOLD,X,Y,Z,XOLD,YOLD,ZOLD,WATE,OLDWT,WTBC,BLZNT,BLZON,AGE,OLDAGE
C * * * check for fission region * * *
      IF(NMED.ne.1)RETURN
C * * * calculate fluence estimate
      TRK = WTBC * SQRT((X-XOLD)**2 + (Y-YOLD)**2 + (Z-ZOLD)**2)
C  * * * sum track lemgth in this medium
C  * * *
c  * * *  Find which shell collision occurs in
      RAD=SQRT(X**2 + Y**2)
      rad1=85.688
      rad2=121.178
      rad3=148.412
      rad4=171.371
      rad5=191.599
      rad6=209.886
      rad7=226.703
      rad8=242.356
      rad9=257.057
      rad10=270.965
      if(RAD.le.rad1) ndetec = 1
      if((RAD.le.rad2).and.(RAD.gt.rad1)) ndetec = 2
      if((RAD.le.rad3).and.(RAD.gt.rad2)) ndetec = 3
      if((RAD.le.rad4).and.(RAD.gt.rad3)) ndetec = 4
      if((RAD.le.rad5).and.(RAD.gt.rad4)) ndetec = 5
      if((RAD.le.rad6).and.(RAD.gt.rad5)) ndetec = 6
      if((RAD.le.rad7).and.(RAD.gt.rad6)) ndetec = 7
      if((RAD.le.rad8).and.(RAD.gt.rad7)) ndetec = 8
      if((RAD.le.rad9).and.(RAD.gt.rad8)) ndetec = 9
      if((RAD.le.rad10).and.(RAD.gt.rad9)) ndetec = 10
      CON = TRK
      goto 101
  101 CALL FLUXST(NDETEC,IGO,CON,0.0,0.0,0)
C  *  *  SWITCH =  0  -- STORE IN ALL RELEVANT ARRAYS EXCEPT UD
      RETURN
      END
```

The subroutines TRKBDR and TRKCOL were modified for use in calculating the axial fluence. The remainder of the FORTRAN code was unchanged. These two subroutines are reproduced here :

```
      SUBROUTINE TRKBDR
C*********************************************************************
C   this version sums track length for fluence
C   in cylindrical slabs
C       MEDIA:  1   - fissile fiber pile
C               2   - reflector
```

```
C               3  - Al shell
C            1000 -interior void
C               0 - exterior void
C*****************************************************************
      COMMON /PDET/ ND,NNE,NE,NT,NA,NRESP,NEX,NEXND,NEND,NDNR,NTNR,NTNE,
     1 NANE,NTNDNR,NTNEND,NANEND,LOCRSP,LOCXD,LOCIB,LOCCO,LOCT,LOCUD,
     2 LOCSD,LOCQE,LOCQT,LOCQTE,LOCQAE,LMAX,EFIRST,EGTOP
      COMMON /NUTRON/ NAME,NAMEX,IG,IGO,NMED,MEDOLD,NREG,U,V,W,UOLD,VOLD
     1 ,WOLD,X,Y,Z,XOLD,YOLD,ZOLD,WATE,OLDWT,WTBC,BLZNT,BLZON,AGE,OLDAGE
C * * * check for neutron not coming from fission region  * * *
      IF(MEDOLD.ne.1)RETURN
C * * * add track length to zone detector * * *
      TRK = WATE * SQRT((X-XOLD)**2 + (Y-YOLD)**2 + (Z-ZOLD)**2)
c  * * *  determine which slab , direction and detector
      RAD = Z
      OLDRAD=ZOLD
      delrad=RAD-OLDRAD
c  * * * Check for particle passing shell to shell
      if(nmed.ne.1) delrad=1
      rad1=54.193
      rad2=108.386
      rad3=162.579
      rad4=216.772
      rad5=270.965
      rad6=325.158
      rad7=379.351
      rad8=433.544
      rad9=487.737
      rad10=541.93
      if(RAD.le.rad1) ndetec = 1
      if((RAD.le.rad2).and.(RAD.gt.rad1)) ndetec=2
      if((RAD.le.rad3).and.(RAD.gt.rad2)) ndetec=3
      if((RAD.le.rad4).and.(RAD.gt.rad3)) ndetec=4
      if((RAD.le.rad5).and.(RAD.gt.rad4)) ndetec=5
      if((RAD.le.rad6).and.(RAD.gt.rad5)) ndetec=6
      if((RAD.le.rad7).and.(RAD.gt.rad6)) ndetec=7
      if((RAD.le.rad8).and.(RAD.gt.rad7)) ndetec=8
      if((RAD.le.rad9).and.(RAD.gt.rad8)) ndetec=9
      if((RAD.le.rad10).and.(RAD.gt.rad9)) ndetec=10
      if (delrad.lt.0) ndetec = ndetec + 1
      CON = TRK
      goto 101
  101 CALL FLUXST(NDETEC,IG,CON,0.0,0.0,0)
C  *  *  SWITCH =  0  -- STORE IN ALL RELEVANT ARRAYS EXCEPT UD
      RETURN
      END
      SUBROUTINE TRKCOL
C*****************************************************************
C   this version sums tracklength within   each              detector
C   volume and is used with TRKBDR (called from BANKR(7))
```

```
C*********************************************************************
      COMMON /PDET/ ND,NNE,NE,NT,NA,NRESP,NEX,NEXND,NEND,NDNR,NTNR,NTNE,
     1 NANE,NTNDNR,NTNEND,NANEND,LOCRSP,LOCXD,LOCIB,LOCCO,LOCT,LOCUD,
     2 LOCSD,LOCQE,LOCQT,LOCQTE,LOCQAE,LMAX,EFIRST,EGTOP
      COMMON /NUTRON/ NAME,NAMEX,IG,IGO,NMED,MEDOLD,NREG,U,V,W,UOLD,VOLD
     1 ,WOLD,X,Y,Z,XOLD,YOLD,ZOLD,WATE,OLDWT,WTBC,BLZNT,BLZON,AGE,OLDAGE
C * * * check for fission region * * *
      IF(NMED.ne.1)RETURN
C * * * calculate fluence estimate
      TRK = WTBC * SQRT((X-XOLD)**2 + (Y-YOLD)**2 + (Z-ZOLD)**2)
C  * * * sum track lemgth in this medium
C  * * *
C  * * *  Find which axial slab collision occurs in
      RAD=Z
      rad1=54.193
      rad2=108.386
      rad3=162.579
      rad4=216.772
      rad5=270.965
      rad6=325.158
      rad7=379.351
      rad8=433.544
      rad9=487.737
      rad10=541.930
      if(RAD.le.rad1) ndetec = 1
      if((RAD.le.rad2).and.(RAD.gt.rad1)) ndetec = 2
      if((RAD.le.rad3).and.(RAD.gt.rad2)) ndetec = 3
      if((RAD.le.rad4).and.(RAD.gt.rad3)) ndetec = 4
      if((RAD.le.rad5).and.(RAD.gt.rad4)) ndetec = 5
      if((RAD.le.rad6).and.(RAD.gt.rad5)) ndetec = 6
      if((RAD.le.rad7).and.(RAD.gt.rad6)) ndetec = 7
      if((RAD.le.rad8).and.(RAD.gt.rad7)) ndetec = 8
      if((RAD.le.rad9).and.(RAD.gt.rad8)) ndetec = 9
      if((RAD.le.rad10).and.(RAD.gt.rad9)) ndetec = 10
      CON = TRK
      goto 101
  101 CALL FLUXST(NDETEC,IGO,CON,0.0,0.0,0)
C  *  *  SWITCH =  0  -- STORE IN ALL RELEVANT ARRAYS EXCEPT UD
      RETURN
      END
```

Appendix B Spacecraft Mission Model

The following equations, solved on TK Solver Plus, were used to model the performance of the $\bar{p}$-FFR :

```
" FFR3.TK  He reaction mass FF rocket
"
C me=AWfuel*Camukg
C Edot=x*pdot*nff*2*KEff
C Ee=1.5*k*Temp
C Ee=.5*me*(ve^2)/1.6e-13
C Nedot=Edot/Ee
C mdot=Nedot*me
C Mfuel=mdot*t
C Men=Msh+Mu+Mpsto
C Mss=Mpl+Men+(.5*Mfuel)
* DeltaV=Mfuel*ve/Mss
C Npbar=pdot*t
```

The following variable definitions are used in the spacecraft mission model. Sample values are shown for a ΔV calculation :

L	2562058	Mss		Spaceship Total Mass
L	4951366	Mfuel		Fuel Total Mass (ejecta)
L		DeltaV	7313.9014	m/s
	1E16	pdot		P-bars per second
	8	x		Multiplication
		Npbar	3E23	Total Number of P-bars
L	4000	Temp		Temperature of ejecta (K)
	3E7	t		time of thrust (s)
L	.16504553	mdot		Mass flow rate (kg/s)
L	3784.5394	ve		Ejecta Velocity (m/s)
L	2.9739E-7	Ee		Energy per ejecta particle (MeV)
	6.644E-27	me		mass of ejecta/particle (kg)
	7.3872E18	Edot		Energy delivered/sec (Mev)
	.54	nff		FF extraction efficiency
L	2.484E25	Nedot		Number ejected part/sec
	75000	Msh		Shield Mass
	375	Mu		Uranium Total Mass
	1000	Mpsto		P-bar Storage Mass
	76375	Men		Engine Total Mass
	10000	Mpl		Payload Mass
	8.62E-11	k		Boltzmans constant
	4.0026	AWfuel		Atomic Weight of fuel
	85.5	KEff		KE per FF
	1.66E-27	Camukg		kg/AMU
	6.022E23	NA		#/mol

Bibliography

Brewer, Donald A., Editor. Space Handbook. Air University Institute for Professional Development Publication AUIPD-1, Maxwell Air Force Base, Alabama, July, 1968.

Chapline, George and Yoshiyuki Matsuda. Energy Production Using Fission Fragment Rockets. Lawrence Livermore National Laboratory Report UCRL-JC-107357, August, 1991.

Cramer, S.N. Applications Guide to the MORSE Monte Carlo Code. Oak Ridge National Laboratory Technical Manual ORNL/TM-9355, Oak Ridge, Tennessee, August, 1985.

Emmett, M.B. The MORSE Monte Carlo Radiation Transport Code System. Oak Ridge National Laboratory, ORNL 4972/R2, Oak Rodge Tennessee, July 1984.

Forward, R.L. Antiproton Annihilation Propulsion. Air Force Rocket Propulsion Laboratory Report AFRPL TR-85-034, September, 1985.

Forward, R.L. Advanced Space Propulsion Study. Air Force Rocket Propulsion Laboratory Report AFRPL TR-87-070, October, 1987.

Frank, W.H. and others. Introduction to TK Solver Plus. Universal technical Systems, Rockford, Illinois, 1988.

Glasstone, Samuel and Philip J. Dolan. The Effects of Nuclear Weapons. U.S. Government Printing Office, 1977.

Ingersoll, D.T. and others. DABL69: A Broad-Group Neutron/Photon Cross-Section Library for Defense Nuclear Applications. Oak Ridge National Laboratory, ORNL/TM-10568, 1989.

Lewis, R.A. and others. Antiproton Boosted Microfission. Pennsylvania State University Report PSU LEPS 91/07, June, 1991.

Morgan, D.L. Jr. Annihilation of Antiprotons in Heavy Nuclei. Air Force Rocket Propulsion Laboratory Report AFRPL TR-86-011, April 1986.

Rich, Arthur. "Antihydrogen Production," Proceedings of the 10 May 1989 Antiproton Technology Workshop. 97-113. Astronautics Laboratory Report AL-CP-89-01, May, 1989.

Schnitzler, Bruce G. and others. Fission Fragment Rocket Scientific Feasibility Assessment. Idaho National Engineering Laboratory Report EGG-NERD--8585, June, 1989.

Smith, Gerald A, Professor of Physics. Correspondence to Maj. Denis Beller. The Pennsylvania State University, University Park, PA, 05 November, 1991a.

-----. Correspondence to Maj. Denis Beller. The Pennsylvania State University, University Park, Pennsylvania, 08 October, 1991b.

-----. Telephone interview. The Pennsylvania State University, University Park, Pennsylvania, 02 October, 1991c.

-----. "Preliminary Report of Results, October 14, 1988 - October 13, 1990." A Report of Activities on JPL Contract 958301, Jet Propulsion Laboratory, Pasadena, California, August 16, 1990.

Weast, Robert C. and others. CRC Handbook of Chemistry and Physics, 67th Edition. Boca Raton, Florida: CRC Press, Inc., 1986.

Yemel'yanov, V.S. and A.I. Yevstyukhin. The Metallurgy of Nuclear Fuel. Oxford: Permagon Press, 1969.